

## Rotary jet spinning review – a potential high yield future for polymer nanofibers

James J. Rogalski, Cees W. M. Bastiaansen & Ton Peijs

To cite this article: James J. Rogalski, Cees W. M. Bastiaansen & Ton Peijs (2017) Rotary jet spinning review – a potential high yield future for polymer nanofibers, *Nanocomposites*, 3:4, 97-121, DOI: [10.1080/20550324.2017.1393919](https://doi.org/10.1080/20550324.2017.1393919)

To link to this article: <https://doi.org/10.1080/20550324.2017.1393919>



© 2017 The Author(s). Published by Informa UK Limited, trading as Taylor & Francis Group



Published online: 01 Dec 2017.



Submit your article to this journal [↗](#)



Article views: 3360



View related articles [↗](#)



View Crossmark data [↗](#)



Citing articles: 23 View citing articles [↗](#)

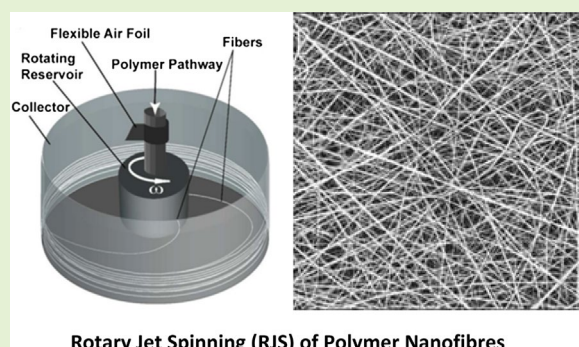


# Rotary jet spinning review – a potential high yield future for polymer nanofibers

James J. Rogalski, Cees W. M. Bastiaansen and Ton Peijs\*

School of Engineering and Materials Science, and Materials Research Institute, Queen Mary University of London, Mile End Road, E1 4NS London, UK

**Abstract** Polymeric nanofibers have been the focus of much research due to their continually evolving applications in fields such as biomedicine, tissue engineering, composites, filtration, battery separators, and energy storage. Although several methods of producing nanofibers have shown promise for large scale production, none have yet produced large enough volumes at a low cost to be the front runner in the field, and therefore the preferred choice for industrialization. Rotary jet spinning (RJS) could be the answer to high throughput, low cost, and environmentally friendly nanofiber production. Being exploited in only the last decade, it is a technology that has seen relatively little research, but one which could potentially be the answer to large scale manufacturing of polymer nanofibers. In this review, we focus on fundamental processing characteristics and initial application driven research. A comparison between existing nanofiber production methods is drawn with the key differences noted. Two methods of utilizing RJS in nanofiber production are discussed, namely spinning from a polymer melt, and solution-based spinning as is typically used in more traditional methods such as electrospinning. Modeling of the process is introduced, in which material selection and processing parameters play an important role.



Rotary Jet Spinning (RJS) of Polymer Nanofibers

**Keywords** Polymer nanofibers, Rotary jet spinning, Electrospinning, Processing, Properties, Applications, Modeling

**Cite this article** James J. Rogalski, Cees W. M. Bastiaansen and Ton Peijs; Nanocomposites, doi: [10.1080/20550324.2017.1393919](https://doi.org/10.1080/20550324.2017.1393919)

## Introduction

Polymer nanofiber research is a topical field in the materials world today<sup>1</sup> and is made up of many different types of production and assembly methods based around the development and pace of the technology being introduced. Within each novel way of manufacturing nanofibers, a myriad of uses for each type exists. It is this demand for varying uses which provides the driving force behind the research into newer, better technologies. Each new iteration or technology jump tries to overcome the flaws of their predecessors. This constant innovation and continuing research is looking toward the use of nanofibers to complement the existing burgeoning microfiber industry. Nanofibers, which are fibers typically less than one micrometer in diameter, are slowly being introduced into the market as technologies to successfully manufacture them in large volumes become available.

The manufacturing techniques that are available to produce nanofibers, as well as microfibers, vary greatly, with some techniques offering benefits that supersede others in either volume, cost, or environmental qualities, etc. While some

techniques produce vast amounts of material in a short space of time, others are only capable of producing insignificant amounts not suitable for industrial scale applications.

## Why polymer nanofibers?

There exist many reasons why it is beneficial for certain applications to prefer nanofibers over microfibers, largely due to their ability to offer advantages due to their reduced diameter. Within this nanoscale, the fibers have a greater surface area to volume ratio and tunable porosity,<sup>2</sup> making them attractive for applications such as filtration and composites, where filters may benefit from increased efficiency by reducing the fiber diameter,<sup>3</sup> and nanocomposites may show potentially enhanced properties, notably toughness, due to an increase in surface area.<sup>4-6</sup> In a typical filtration application of nanofiber mats as can be seen in Figure 1, the pollen spore is incapable of traveling through the nanofiber mat, rendering it a suitable air filtration application for a variety of objects (Figure 2).

Currently, nanoscale fibers can be produced using existing techniques such as electrospinning,<sup>8-10</sup> melt blowing,<sup>11,12</sup> island-in-the-sea spinning<sup>13-15</sup> and template synthesis<sup>16</sup> to

\*Corresponding author, email [t.peijs@qmul.ac.uk](mailto:t.peijs@qmul.ac.uk)

© 2017 The Author(s). Published by Informa UK Limited, trading as Taylor & Francis Group.

This is an Open Access article distributed under the terms of the Creative Commons Attribution License (<http://creativecommons.org/licenses/by/4.0/>), which permits unrestricted use, distribution, and reproduction in any medium, provided the original work is properly cited.

Received 19 July 2017; accepted 13 October 2017

DOI: [10.1080/20550324.2017.1393919](https://doi.org/10.1080/20550324.2017.1393919)

name a few. These methods and others like them, which will only be described in limited detail in this review, have been the primary method of nanofiber production for some time. There exist drawbacks to many of these methods, be it low production rates or having to using large quantities of energy for fiber production. A more efficient method is needed to create nanofibers which would increase production rates and reduce power consumption. One such method that could answer these requirements is rotary jet spinning (RJS).

## Introduction to rotary jet spinning

RJS is known by a few names within the research community; however, the RJS title sums up the process better than most, and will be used in this review. RJS is also known as centrifugal spinning, rotor spinning, and Forcespinning™. This last

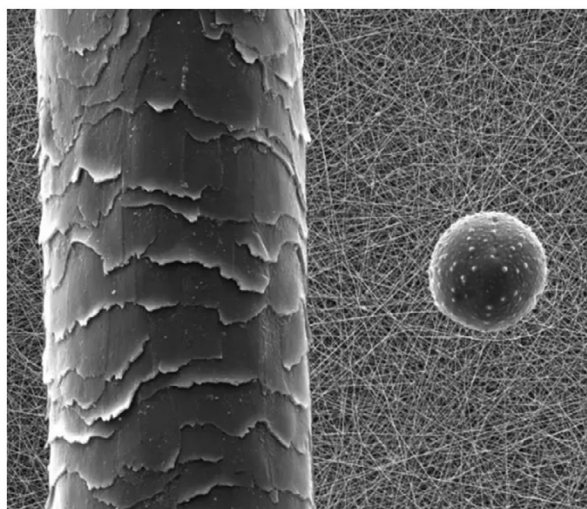


**Figure 1** Nanofiber scale (human hair, pollen grain, nanofiber mat). Photograph courtesy of Elmarco [7]

term was introduced as a brand name by FibeRio® Technology Co. (Acquired by Clarcor Inc. in 2016, who were subsequently acquired by Parker Hannifin in 2017), for what appeared to be the only commercial enterprise specializing in the development and production of RJS machinery on the market. It was at the University of Texas where the initial patents were filed by Lozano and Sarkar before being commercialized by FibeRio.<sup>17,18</sup>

Since the granting of FibeRio's RJS patents in the last decade,<sup>17,19–25</sup> a flurry of research relating to this field has started to emerge. Around a third of publications utilizing RJS as a primary nanofiber production method have used equipment produced by FibeRio in some way, but the majority do not, opting to create their own RJS machines instead. Although the mechanics behind RJS are simple, and resemble candy floss making machines that have been around for decades, developing a device that is capable of precision control for the benefit of tunable fiber morphology is key.

To gage the scale of recent interest in centrifugally spun fibers, results from a patent search into characteristic patent code D01D 5/18, which classifies any patent relating to natural or artificial threads or fibers created by means of rotating spinners, shows an increase in the filing of patents since the year 2000 (Figure 3). Under this classification, which is included as one of multiple classifications in a patent registration, all the equipment or processes that are being patented are directly related to polymer nanofiber manufacturing or applications.

More patent categories exist which give an overview of the rise of this technology, however this classification code search depicts the trend well enough to consider only one type for illustration purposes.

The highest number of patent registrations come from China and the United States (Table 1), with a steady rise in patents relating to fiber spinning occurring since 2007, with a slight reduction from both the USA and China in 2012 and 2013. Recent years account for the highest registrations, indicating a continued

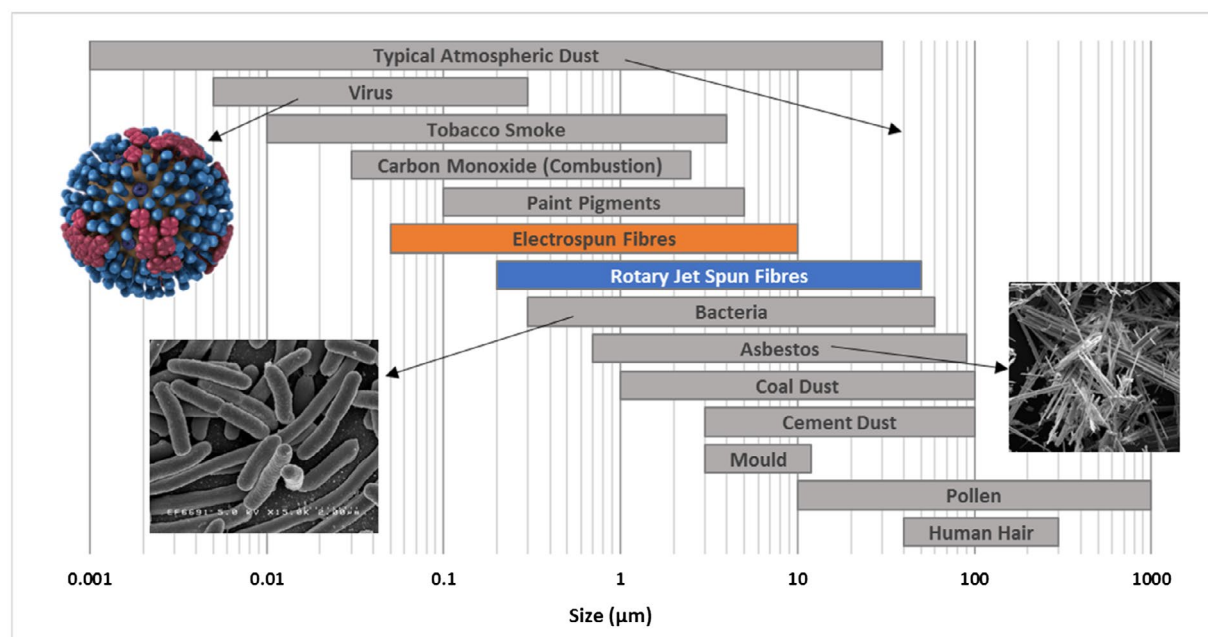


**Figure 2** Comparison of the sizes of typical objects relevant for air filtration with fiber diameters of RJS and electrospun (ES) fibers

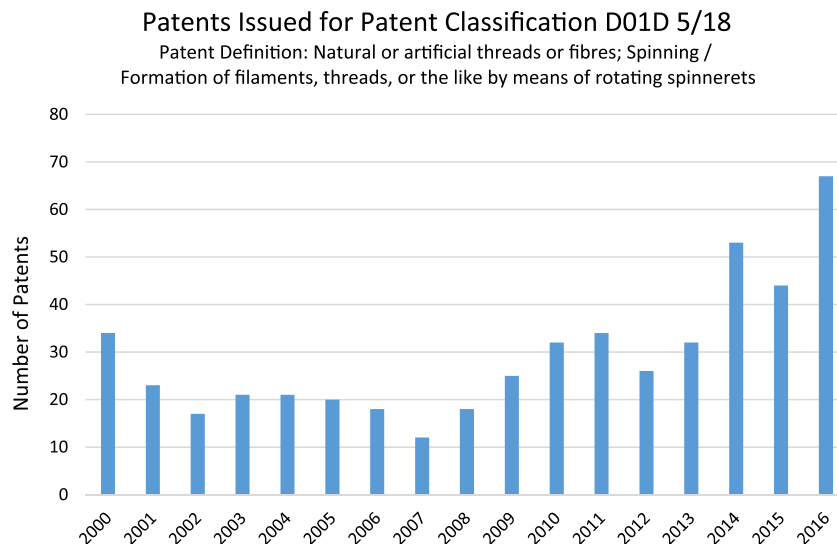


**Figure 3** Patents issued for fiber creation relating to rotating spinnerets since 2000. Data compiled from Espacenet.com.<sup>26</sup>

**Table 1** List of countries with the highest number of patents filed for devices relating to the manufacture of fibers from rotating spinnerets from 2000 to 2016

Country	Total
China	126
United States of America	88
Korea (South)	56
World Intellectual Property Organization (WIPO)	50
Japan	39
European Patent Office	35
Germany	16
Spain	13
Austria	10
Canada	9
Australia	7

interest in the technology, with 2016 being the largest number to date.

Publications relating directly to RJS, the primary focus of this review, can be seen in Figure 4. These illustrate the number of scientific publications per year according to Web of Science (WoS) since this technology started to gain traction.

The fundamental principle behind RJS is relatively straightforward although the technology does require some knowledge of polymer chemistry, processing, and fluid mechanics. The basic concept of RJS is illustrated in Figure 5 and is, as mentioned earlier, not too dissimilar to the well-known method used in the catering industry for the manufacture of candy floss.

Basic requirements in RJS are a reservoir to hold the polymer, which is in either solution or melt form, and a nozzle through which the polymer is spun once it is rotated at a high enough angular velocity to initiate jet expulsion. In addition to this, a collector to “catch” the fibers after they are spun and stretched in the air vortices as they make their way from the nozzle is also needed. This can take many forms, but the most common method used is a radial array of vertical collector bars.

## Comparisons with other techniques

Many techniques other than RJS can be used to create polymeric nanofibers, but none with as high capacity for industrial

scaling using such low power consumption. Other nanofiber production methods include drawing,<sup>27,28</sup> template synthesis,<sup>16,29,30</sup> phase separation,<sup>31</sup> self-assembly,<sup>32–34</sup> islands in the sea,<sup>14,35</sup> electrospinning,<sup>8–10,36–41</sup> and melt-blown spinning.<sup>12,42–44</sup> Each of these processes has distinct advantages and disadvantages, which have been summarized by Nayak et al.<sup>45</sup> and are presented in Table 2.

Although RJS is sometimes labeled as environmentally friendly, the process can only be credited as such if the solvent is recycled or not used at all, such as with melt RJS. However, alternative methods used to produce fibers from the melt can use significantly more energy, thus making them less environmentally friendly. In all of these melt processing techniques thermal degradation is a possibility, but can be overcome by using thermal stabilizers.<sup>46</sup>

## Electrospinning

Electrospinning (ES) is a method that relies on an electrostatic force to spin a fiber from a polymer solution droplet suspended from a capillary by overcoming the surface tension in the droplet to form fibers on a counter electrode.<sup>39,47–51</sup> This can be conducted through a single needle approach (Figure 6), or multiple needles can be used to increase production rate of fibers. Needleless systems such as Elmarco’s Nanospider™ technology also exist, allowing semi-industrialized volumes of fiber to be produced on a scale of  $<200 \text{ g h}^{-1}$  using polyvinyl alcohol (PVA) for example.<sup>7,50</sup>

When comparing electrospinning with RJS, we can demonstrate the variance in parameters such as fiber diameter with some ease. In comparing the production of poly(ethylene oxide) (PEO) fibers from these two systems, similarity can be gaged and discussed. Son et al.<sup>52</sup> produced beadless nanofibers through the electrospinning of a PEO/water solution at concentrations of 3, 4 and 7 wt%. The average fiber diameters were between 0.36 and 1.96  $\mu\text{m}$ , with the larger diameters a result of other solvents such as ethanol, chloroform, and DMF. This can be directly compared with PEO/water solutions ranging between 6 and 10 wt% produced by Padron et al. using



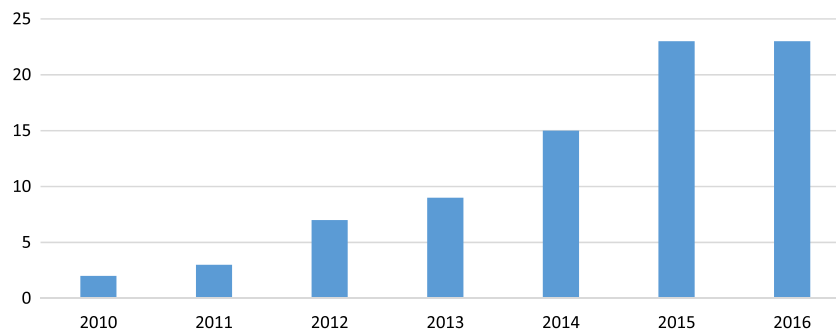


Figure 4 RJS publications by year 2010–2016 according to WoS

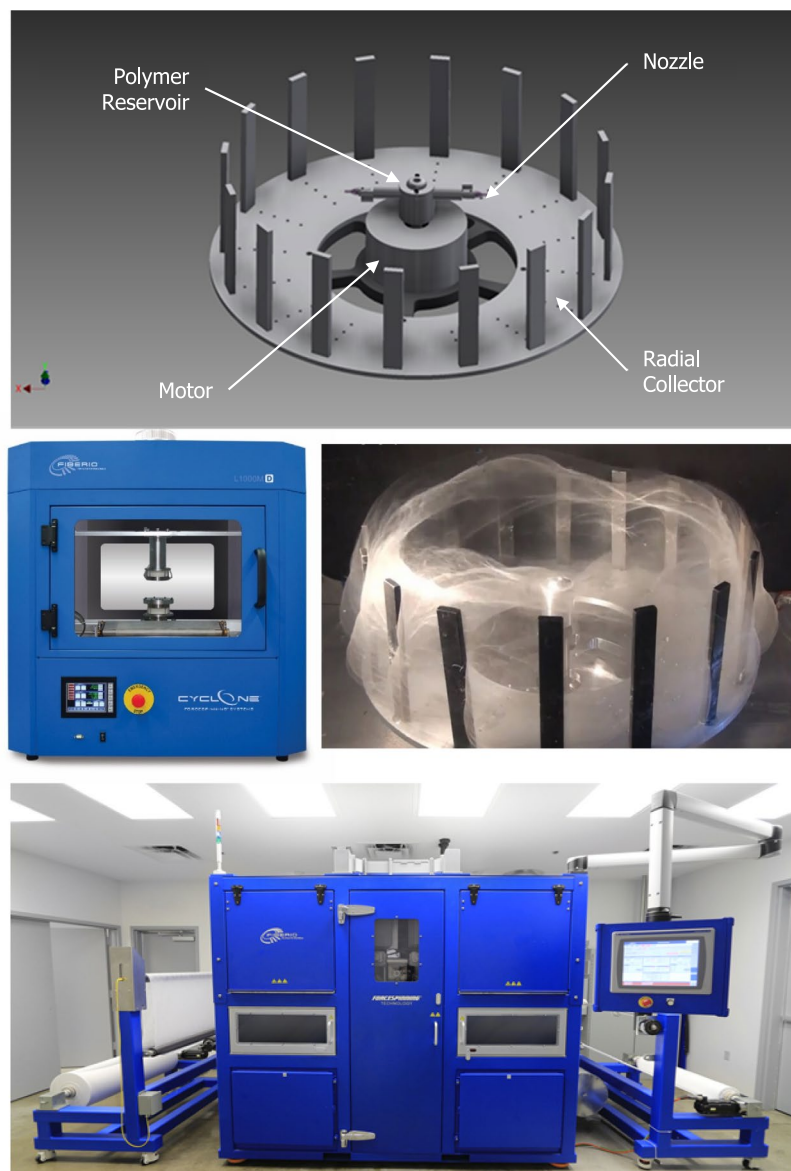
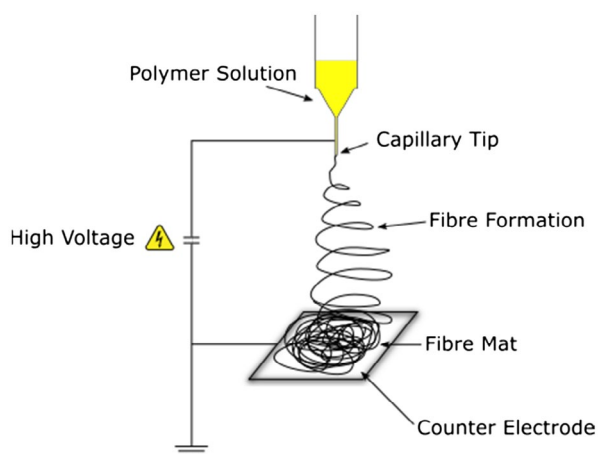


Figure 5 Schematic illustration of rotary jet spinning (RJS), comprised of an electric motor driven rotating spinneret with polymeric fibers being ejected outwards toward the vertical collector bars in this typical setup. Photographs (top left to bottom) of the FibeRio Cyclone™ L1000M laboratory machine, with fiber spinning demonstration, and the Fibre Engine FX System which is configurable for 1.1 m (FX1100) or 2.2 m (FX2200) line widths, achieving an output of up to 200 g/min and compatible with line speeds of up to 200 m/min. Photographs courtesy of FibeRio

**Table 2** List of nanofiber production methods. After Nayak et al.<sup>45</sup>

Manufacturing process	Scope for scaling-up	Repeatability	Control of fiber dimension	Advantages	Disadvantages
Electrospinning (solution)	Yes	Yes	Yes	Long and continuous fibers	Solvent recovery issues, low productivity, jet instability
Electrospinning (melt)	Yes	Yes	Yes	Long and continuous fibers	Thermal degradation of polymers, electric discharge problem
Melt blowing	Yes	Yes	Yes	Long and continuous fibers, high productivity, free from solvent recovery issues	Polymer limitations, thermal degradation of polymers
Island in the sea spinning	Yes	Yes	Yes	Long and continuous, relative uniformity	Solvent recovery and extra processing
Template synthesis	No	Yes	Yes	Easy to vary diameter by using different templates	Complex process
Drawing	No	Yes	No	Simple process	Discontinuous process
Phase-separation	No	Yes	No	Simple equipment required	Only works with selective polymers
Self-assembly	No	Yes	No	Easy to obtain smaller nanofibers	Complex process
Rotary jet spinning	Yes	Yes	Yes	Free from very high voltage, eco-friendly	Requirement of high temperatures



**Figure 6** Typical electrospinning setup showing the polymer solution being delivered through a needle to a capillary tip, before being caught in the electrostatic attraction of the counter electrode, drawing a fiber across the void into the whipping zone before being deposited as a fiber mat

RJS<sup>53</sup> in which fiber diameters obtained were 0.13–0.32  $\mu\text{m}$  dependant on angular velocity of the spinneret. A conclusion can be drawn from this simple comparison that the diameters achievable from electrospinning are comparable to RJS.

## Melt blowing

Although we will not cover all techniques in this review, it is important to compare RJS with other techniques such as melt blowing (Figure 7). This technology utilizes fast flowing heated air and dies to extrude a polymer melt, where after the produced fiber is carried along in the stream of hot air, which is typically the same temperature as the die, before being deposited on a collection device.<sup>11</sup> This stream of heated air flows at very high velocities which is very energy consuming due to the high velocity and temperatures which are required.<sup>42</sup>

## Other methods

Template synthesis is a method that consists of creating nanowires by filling a porous template that contains a large number of straight cylindrical holes with a narrow size distribution. Although scientifically interesting, it is however not suited for large-scale industrial production.<sup>16</sup> Drawing, phase separation and self-assembly are also not suitable for large-scale applications and will not be discussed further here as a comparison to RJS.

The island-in-the-sea method of nanofiber creation is however a method that can be scaled toward mass production, but does not produce continuous fibers. It is based on the use of two incompatible polymers which are melt blended together to form a morphology replicating that of islands in the sea, where the islands are the nanofibers and the sea is the sacrificial matrix used to aid in the drawing of the fibers.<sup>55</sup>

## Efficiency and yield

RJS shows promise toward market adaptability when combined with considerations such as energy efficiency. In RJS we do not require the high voltages that come with electrospinning or the high velocity air jets that are required in melt blowing – both of which are relatively large contributors to the overall cost of fiber production. Another benefit afforded to RJS is that (when melt spinning) we do not have to rely on the use of harmful solvents, resulting in a “greener” product – a feature which is however also possible with most other fiber production methods.

Lab scale versions of RJS machines can already produce more than 50 times the rate (60 g h<sup>-1</sup> per orifice<sup>53</sup> vs. 0.11 g h<sup>-150,53</sup>) of a single needle lab scale electrospinning setup if only comparing one orifice. The standard number of orifices on a RJS machine would be at least 2, some with many more, dependant on design, meaning a 100 fold increase in production rate for a lab scale RJS machine over a single needle electrospinning machine. RJS spinnerets can in turn be

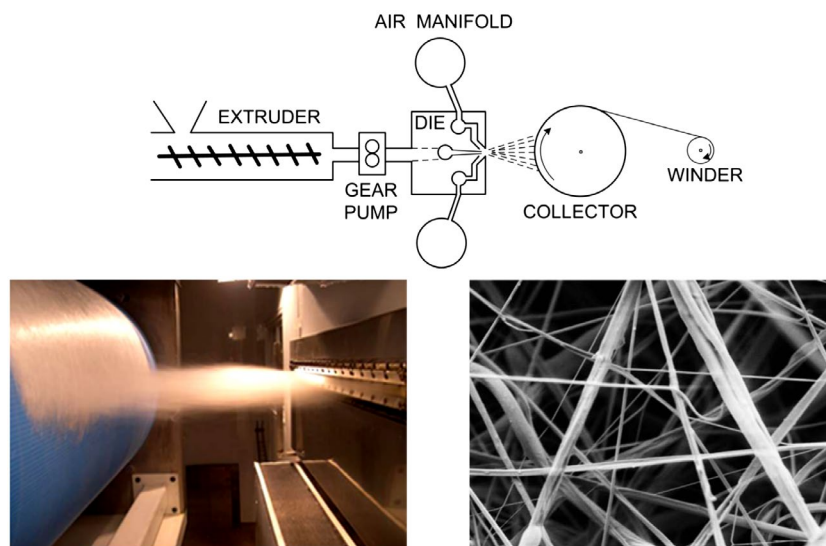


**Figure 7** Schematic of the melt blowing process where heated air moves at speed past a polymer melt to create fibers (top). Image of the melt blowing process and produced fiber. Reprinted from Hiremath and Bhat,<sup>54</sup> available under a Creative Commons attribution 3.0 license

**Table 3** Industrial nanofiber production system comparison, showing manufacturer's quoted production rates of continuous nanofiber deposition on substrates, with the FX2200 RJS system being the highest

Manufacturer	Output width (mm)	Quoted production rates
Nanospider™ (NS 8S1600U) by Elmarco (Czech Rep.)	1600	78 g h <sup>-1</sup> 1680 m h <sup>-1</sup> 2640 m <sup>2</sup> h <sup>-157</sup>
NW-101 by MECC Co. Ltd (Japan)	600	600 m h <sup>-158</sup>
Nanospinner416 by inovenso (Turkey)	1000	210 g h <sup>-1</sup> 210 m <sup>2</sup> h <sup>-159</sup>
SPIN line by SPUR® (Czech Rep.)	1200	186 g h <sup>-1</sup> 300 m <sup>2</sup> h <sup>-160</sup>
Fluidnatek LE-1000 by Bioinicia (Spain)	3000	Not available
FX2200 by Fiber-Rio (US)	2200	12,000 g h <sup>-1</sup> 12,000 m h <sup>-156</sup>

positioned in parallel to create a system which covers a larger area for creating continuously fed nonwoven mats.

Exploring the production rates of processes capable of producing industrial volumes of nanofibers highlights even more the differences between methods when considering the commercial future of polymer nanofibers. FibeRio's Cyclone™ Fibre Engine FX System, which is designed with a modular and expandable architecture configurable for 1.1 m (FX1100) or 2.2 m (FX2200) line widths, can achieve continuous outputs of up to 12,000 g h<sup>-1</sup> with line speeds of up to 200 m min<sup>-1</sup> and controllable fiber diameters of around 500 nm.<sup>56</sup> In comparison, the highest production rates of the leading electrospinning systems are 210 g h<sup>-1</sup> for inovenso's Nanospinner416 1 m line width needleless electrospinning system, depending on polymer solution used (see Table 3).

In addition to the Nanospider™ needles systems, multi-jet systems have been developed and are now commercialized by companies such as 4SPIN (Czech Republic), MECC Co. Ltd (Japan), inovenso (Turkey), SPUR (Czech Republic), and

Fluidnatek (Spain). These systems are complex to provide direct production rate comparisons for as the manufacturers quote various fiber diameters, polymers, solutions and deposition thicknesses, and in some cases only machine speed capabilities. All systems except the RJS FX2200 are electrospinning machines. The only real alternative contender for micro and nanoscale fiber production is melt blowing, which is capable of production rates of around 1500 g h<sup>-1</sup>,<sup>45</sup> but does not provide continuously uniform fiber diameters in the nano scale.

## Fiber diameters

Figure 8 shows the fiber diameters of published RJS data from a range of studies.<sup>53,61–85</sup> The large variability in diameters is generally due to different processing settings (e.g. rotational velocity, orifice size, temperature) and material characteristics (e.g. viscosity, molar mass), rather than statistical variability. Viscosity affects the fiber diameter in RJS and Figure 8 shows a wide variety of fiber diameters for studies that have reported a range of sizes for certain materials. Where only a small diameter variance is shown, the publication often did not specify an upper and lower diameter range, but rather mentioned only a single value.

These fiber diameters illustrate the typical values that can be achieved with the materials shown. Data shown do not necessarily represent the smallest diameters that are possible with this technology, but are however an indication of what has so far been achieved. Comparing the smallest diameters of 10 materials from RJS and ES indicated that reported diameters for ES are on average around 10% smaller. However, electrospinning has been around for much longer and these smaller diameters could be simply the result of a better understanding of the ES process, rather than some intrinsic limitation of the RJS process. For example, one clear difference can be seen by comparing polyamide 6, where electrospinning has produced fibres in the region of 50–100 nm, whereas rotary jet spinning has only reported diameters as low as 450–500 nm (Figure 8).

There is however a larger variation in the uniformity of fiber diameter in RJS compared with ES. This is shown by Krifa and

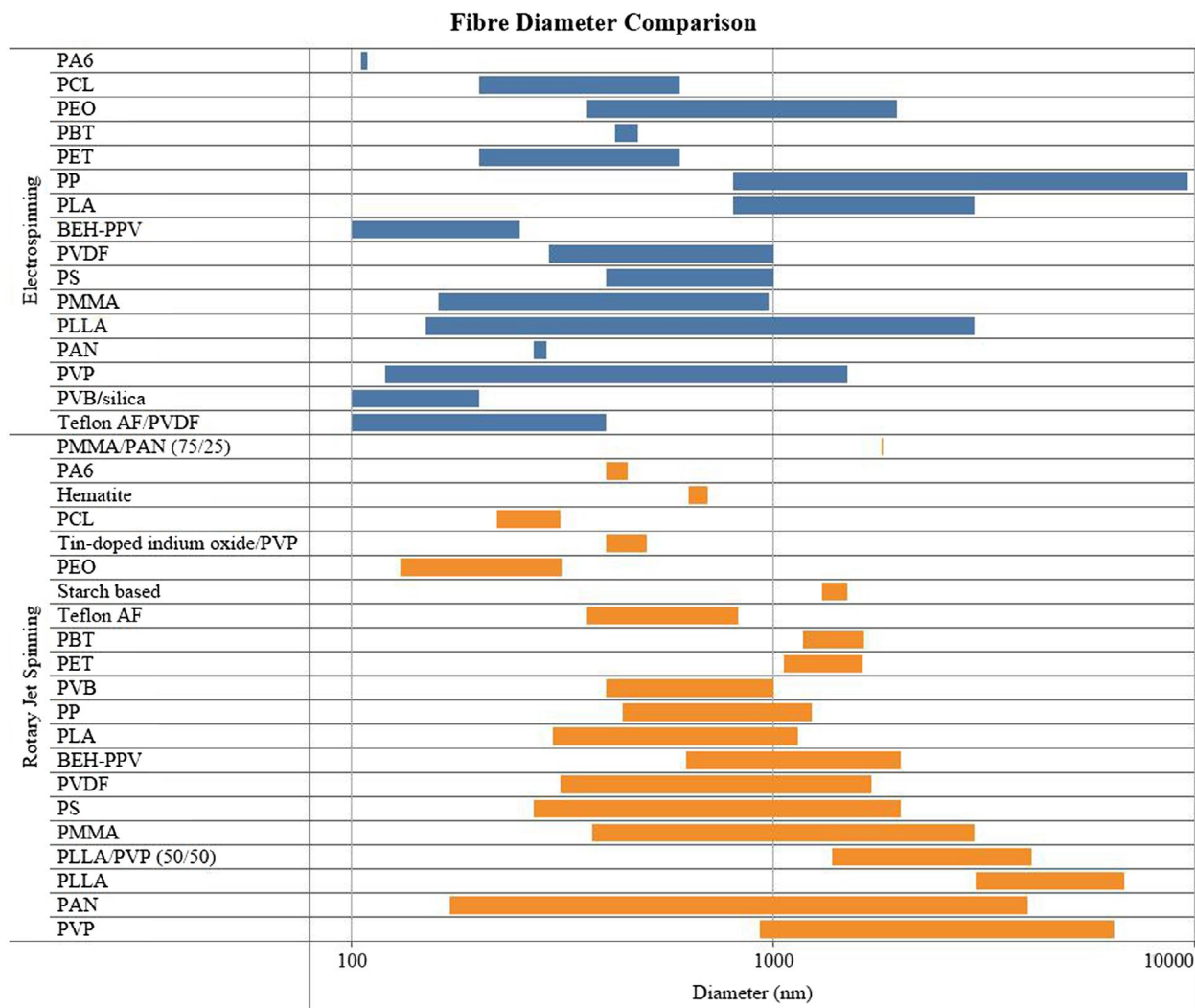


**Figure 8** A comparison of reported fiber diameter ranges for rotary jet spinning<sup>53,61-85</sup> and electrospinning<sup>41,52,86-96</sup>

Yuan,<sup>79</sup> where PA6 fibers spun with properties and processing settings that would guarantee bead free continuous fibers were compared in both electrospinning and RJS (referred to as FS in Figure 9).

The increase and spread in fiber diameters for RJS in comparison to ES can be attributed to, but not limited to, the phenomenon that occurs during the start-up process. For example, in the solution spinning of polycaprolactone (PCL) in dichloromethane (DCM), the first 30 s of RSJ showed a reduction in the fiber diameter to an equilibrium point (Figure 9). Taking these initial larger diameter fibers into account when measuring the average diameter will increase reported values and skew like for like comparisons. In almost all reported RJS fiber diameters, this phenomenon is not considered. It should be noted that the diameters achievable in a continuous RJS device would reach the equilibrium state at a much smaller diameter to that of the start, as demonstrated below.

## Potential nanofiber applications

The fiber industry is a global marketplace with many manufacturers having a large stake in the industry. The industry sub category of nonwoven filter media is a contributor, with

market growth increasing from \$3.7bn in 2013 to \$4.3bn in 2015 alone. With this continued growth, it is predicted to reach \$6.5bn in 2021 which signifies a compound annual growth rate of 7% between 2016 and 2021 as per a market report produced by BCC Research.<sup>97</sup> These statistics cover all manufacturing methods related to nonwoven filter media, both micro and nanofiber. Actual data on nanofiber markets alone are not easily available; however, as future applications begin to develop within the marketplace, correlations with the growing microfiber industry should potentially be seen.

## Biomedical

A commonly published nanofiber application in RJS is based around biomedicine. This application exploits the ability of the nanofibers to offer significantly increased surface area to volume ratios than any other material, which is a highly desirable property in this field. Pelipenko et al.<sup>98</sup> describe that these novel materials can be employed in the treatment of various diseases as well as in the field of regenerative medicine. The promise is that biological function lost in host tissues will be able to be restored and maintained by tissue engineering through the use of RJS nanofibers.<sup>99-102</sup> A common goal



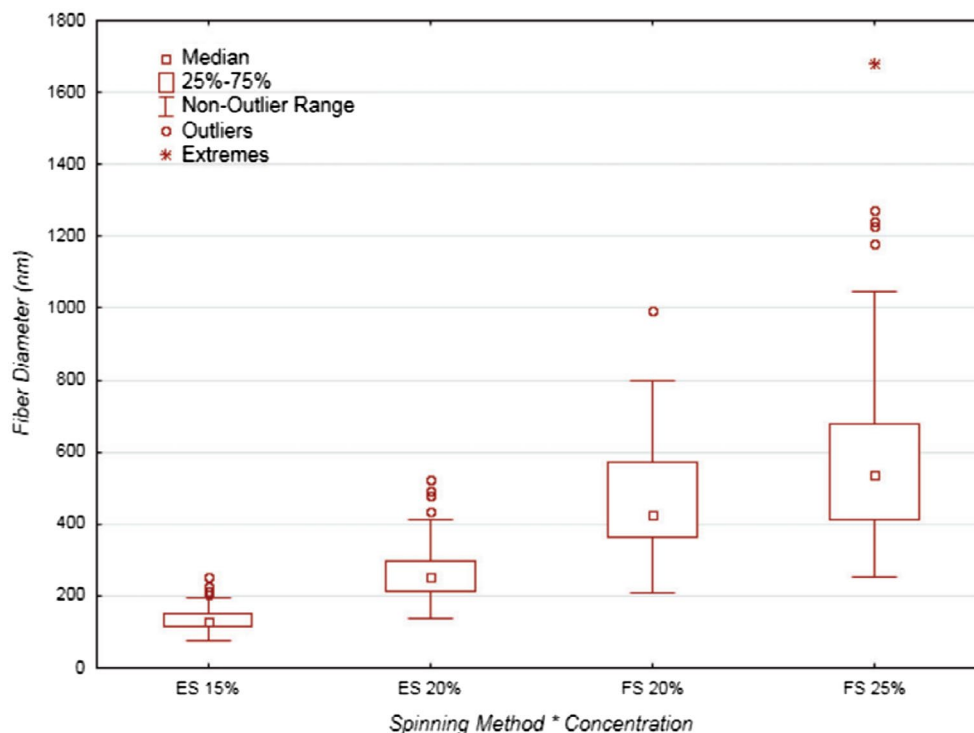


**Figure 9** Comparison of RJS and ES fiber diameter variance, showing a marked increase in the fiber diameter based on polymer concentration in solutions, with RJS showing exponentially higher outliers and extreme values compared with the average. Reprinted with permission from Krifa and Yuan,<sup>79</sup> Copyright 2016, Sage Publications

in the design of tissue engineering scaffolds is to mimic the natural interfaces that interact selectively with a specific cell type through biomolecular recognition.<sup>103,104</sup>

Similar to tissue scaffolds, wound dressings are another biomedical application which has seen much focus, exploiting high surface areas within the nanofibers to foster the perfect conditions for cell growth, embryologic development, organogenesis, and wound repair.<sup>105,106</sup>

Using RJS nanofibers in direct contact with the human body is only one aspect of the biomedical applications of nanofibers. Zhu et al.<sup>107</sup> for example, have investigated affinity absorption materials by functionalizing poly(vinyl alcohol-co-ethylene) (PVA-co-PE) with Cibacron Blue F3GA to evaluate their effectiveness. Affinity membranes can selectively remove bacteria, endotoxins, and viruses from biologically active liquids and water, and if it becomes cheaper to manufacture these types of products, it could benefit developing nations battling against waterborne disease.

Another interesting biological application for RJS nanofibers is that of controlled drug release.<sup>104,108–111</sup> By being able to provide a predictable and controlled drug release over time by exploiting the high volume to surface area of nanofibers, one such study by Wang et al. using RJS has shown that producing aligned fiber mats are preferable when designing for a slower and more controlled release of drugs, rather than a more rapid release for random oriented fibers due to the increased aqueous interaction. In their research, a lab-built device was used to produce polyvinylpyrrolidone (PVP) fibers between 6 and 19 microns in size via electro RJS.<sup>110</sup>

## Nanocomposites

Another interesting application area for nanofibers is their use within nanocomposites. This area has seen research from nanofiber production areas such as electrospinning<sup>112–115</sup> and vapor grown carbon fibers (VGCF)<sup>116,117</sup> in the past, with multiple reviews written on their promising future<sup>4,118–120</sup> Engineering composites typically consist of high modulus (>50 GPa) and high strength (>1 GPa) fibers embedded in a low modulus polymer matrix, which through the interaction between the two, leads to improved mechanical properties of both materials to a level more than which would be expected from each material individually. Increased mechanical strength from nanofibers will be a requirement should nanofiber based composites be successful, with only limited success seen to date as reviewed in detail by Yao et al.<sup>8</sup> and Peijs.<sup>121</sup> Various polymeric materials have been trialed as composite reinforcement, with higher modulus materials such as glass<sup>115,122</sup> and carbon<sup>115,123</sup> nanofibers being among them. Polymer nanofibers, most often produced by electrospinning, typically have Young's moduli of less than 3 GPa and tensile strengths below 300 MPa,<sup>8</sup> which renders them rather ineffective as reinforcement for bulk engineering plastics such as epoxies, polyesters, polyamides, or polypropylenes.<sup>121</sup> However, it has been shown that such fibers can be effective as reinforcements for biomedical engineering purposes when combined with hydrogels.<sup>124</sup>

Manufacturing fibers in the nano scale is of great interest for composites, as these fibers have a high aspect ratio and large available fiber surface area, potentially leading to high

energy absorption mechanisms through debonding and pull-out. As a simple example, a 10  $\mu\text{m}$  diameter microfiber has the same cross sectional area as 10,000 nanofibers with diameter 100 nm – resulting in much more surface area to interact with a composite matrix to aid in energy absorption processes as mentioned above.<sup>125</sup>

Papkov et al.<sup>126</sup> found that by reducing the diameter of electrospun polyacrylonitrile (PAN) fibers from 2.8  $\mu\text{m}$  to  $\sim 100$  nm increased the elastic modulus from 0.36 to 48 GPa, with the largest increase in fibers below 250 nm (see Figure 15). This increase was also commented on by Yao et al.<sup>8</sup> in their review of high strength and high modulus electrospun nanofibers, where it is noted that this is not the only method of achieving increased mechanical properties. Flexible chain polymers generally achieve chain alignment (and thereby higher modulus and strength) through post-drawing, whereas rigid-chain polymers offer the ability to chemically guarantee higher chain alignment during the spinning process.

Two examples of rigid chain polymers being used to produce high mechanical strength nanofibers for use in composites has been investigated using poly(*p*-phenylene terephthalamide)<sup>38</sup> and also polyimide.<sup>127</sup> A composite of electrospun co-polyimide nanofibers within a styrene-butadiene-styrene (SBS) triblock copolymer (Kraton<sup>®</sup>) matrix was produced, where a Young's modulus ranging from 2.5 to 7 GPa was achieved for fiber volume fractions ranging from 21 to 62%, respectively. These values were in good agreement with predictions made using the rule of mixtures.<sup>127</sup> For this, the fiber orientation in the composite laminates was measured, showing an average misalignment angle of 14°. By back calculating the values obtainable for a fully aligned fiber mat a Young's modulus of 26.5 GPa was estimated for a perfectly aligned UD laminate, yielding a co-polyimide fiber modulus of around 60 GPa, similar to commercial high-performance fibers like Kevlar 29.

During electrospinning, albeit on a smaller scale, it is possible to obtain good levels of fiber alignment using the rotating disc method, but an equivalent of such method has not been produced for RJS yet. Badrossamay et al.,<sup>128</sup> Erickson et al.<sup>129</sup> and Wang et al.<sup>110</sup> have developed their own RJS systems to produce aligned fibers, although these studies combined both electrospinning and RJS to achieve this. No reported study has yet achieved a high level of fiber alignment using RJS alone.

## Filtration media

The physical separation of matter occurs predominantly in one of two methods, filtration or sedimentation. Fibers work extremely well when it comes to filtration in order to separate matter, as they are able to be scaled according to the size required. The size of the nonwoven fiber mat porosity required depends on the droplet or particle size that needs to be prohibited from passing through. Filters can be made of many materials, with the most common being natural fibers, synthetic polymers, metals, carbon, ceramics, and paper-like materials.<sup>130</sup>

A typical high performance filter such as a high efficiency particulate air (HEPA) filter is required to have a minimum removal efficiency of 99.97% of particles greater than or

equal to 300 nm in diameter in an air flow rate between 3 and 10  $\text{m s}^{-1}$  (as defined by the United States Department of Energy, DoE, or a range between 85 and 99.999995% in Europe (European Norm EN 1822:2009)). There is also a specification of minimal pressure drop over the filter of around 300 Pa.

Fiber-based filters are at the low to mid-range price compared to other materials such as paper, with new technologies such as RJS hoping to introduce new methodologies for old technologies, with the intention of potentially reducing the sale price to market. According to data published in the *Filters and Filtration Handbook*,<sup>130</sup> the retail price of spunbound fiber filters range from \$0.065 to \$6.50/ $\text{m}^2$ , whereas paper filters are the cheapest at \$0.20 to \$0.33/ $\text{m}^2$ .

Among the most prominent concerns when developing filtration media is the ability of the filter to maintain its usefulness and prevent further harm to users when used as an air filtration device. Because polymer nanofibers are continuous, there is very little chance of them becoming airborne and entering the body. In addition to this benefit, a primary advantage of using nanofibers in filtration applications is their high surface to volume ratio which increases particulate filtration efficiency, and by nature of the design, results in surface loading instead of depth loading as is typical of other nonwoven substrates.<sup>131</sup> This is achieved by increasing the number of overlapping fibers that exist which will limit the flow of particles by trapping them. Therefore, a smaller diameter and hence more fibers result in a higher ratio of blockage points for traveling particulate matter.

Figure 11 shows a standard HEPA filter test of varying air flow rates conducted on polyamide (PA) 6 nanofiber mats, comparing with the industry standard HEPA filter.<sup>132</sup> Samples 1 and 2 were 10 and 5 times thinner, respectively, than the standard HEPA filter being tested, and pressure drop data suggested that the HEPA filter had the lowest pressure drop compared to the PA6 filters. Although this shows superior efficiency from the HEPA filter, the potential to use significantly less material in the PA6 filter versus the HEPA filter, for similar filtration efficiencies, is promising.

A real world study of nanofibers for use in air filtration was conducted at Kaufman North Pit in Clearfield County, Pennsylvania, USA, where a mining vehicle had a comparable cellulose filter tested against a cellulose + nanofiber filter.<sup>3</sup> The result was a reduction in dust particles from 86 to 93%, concluding in a successful trial of the retrofitted nanofiber air filters.

In an attempt to improve the efficiency of filters, Podgorski et al. demonstrated that there is an increase of up to 2.6 times the quality factor (QF) of nanofiber-based filters versus those created using microfibers.<sup>133</sup> QF is a method to evaluate filter performance by measuring the filter efficiency as well as the pressure drop over the filter.

## Additional potential applications

Although a subset of potential nanofiber applications has already been listed, it is important to note a few more which are currently being researched. One such application, in a bid to improve sensor technology, is in the development of polyaniline (PANI) nanofiber gas sensors by utilizing the ability of conducting polymers to display a

transition between insulating and conducting states which may occur due to chemical treatments with redox agents. This method can be used to develop optical, chemical, and biosensors.<sup>134</sup>

Flexible solar cell technology has been investigated by creating nanostructured films from poly(3-hexylthiophene) fibers by mixing them with a molecular acceptor such as [6,6]-phenyl C61-butyric acid methyl ester in solution. By using this process, one could produce an efficient layer of an organic solar cell.<sup>135</sup>

Further potential applications being studied include supercapacitors based on flexible graphene/polyaniline nanofiber composite films [136], graphene/polyaniline nanofiber composites as supercapacitor electrodes,<sup>137</sup> lithium-ion battery separators from PAN,<sup>77,138</sup> polystyrene (PS) nonwoven fabrics featuring radiation induced color changes,<sup>139</sup> nanofiber hydrophilic studies<sup>70,140,141</sup> and anionic dye adsorption techniques [142] to name but a few.

## Materials used in rotary jet spinning

Many polymeric materials have been considered for RJS of nanofibers, with material choice driven by specific fiber characteristics stemming from research goals or end-user applications. Applications and future research directions into nanofibers including RJS fibers are attributed to a few key areas of interest, namely filtration,<sup>3</sup> healthcare, environmental engineering, biotechnology, composites,<sup>121</sup> defense and security and the energy sectors.<sup>143</sup>

Many researchers have started studies into RJS nanofibers driven by applications within specific sectors such as medicine, where fibers resemble cellular topographies<sup>63</sup> or are capable of targeted outcomes such as drug delivery.<sup>68</sup> Others have focused on using conjugated polymers in the RJS process for areas such as photovoltaic cells, light-emitting diodes, and biocompatible materials.<sup>64</sup> The fibers that are created for these purposes are spun from either a melt state or a solution state, all of which are listed below.

## Solution spinning materials

As a relatively new technique for producing fibers, RJS is still undergoing an interesting period of initial research, whereby the materials that are being selected are seemingly either for general research into the RJS technique itself, or they target potential end use applications. The materials chosen are for a relatively broad range of potential applications, but the most common theme amongst specific research is in the field of biomedicine (see Table 4).

In these studies, the fibers produced were evaluated in one of two ways. Firstly, in terms of the RJS process, and secondly in the specific capability toward an intended application. The results showed that application specific publications found favorable quantitative results based on initial objectives, while publications which focused more on the general process of RJS mainly focused on diameters or physical properties of fibers to further understand the RJS process. Several, more recent publications on RJS have continued to focus on processing and application specific research.<sup>15,47,104,106,138,142,158–167</sup>

## Melt spinning materials

Conversely to solution spinning and like electrospinning, RJS in the melt phase has not seen as much research due to the difficulty in processing fibers from the relatively viscous melt (see Table 5). There is unfortunately very little information on unpublished or failed experiments in RJS and thus on materials which did not work. As literature suggests, melt spinning would seem to be more limited in the materials choices facing it, with only a few materials available in the list below from published works:

In the publications listed in Table 5, three were using RJS with a very specific application in mind, while the others were studies of the RJS process itself for specific polymers. These specific application focused studies were successfully able to use the RJS process for the creation of tissue scaffolds as well as drug delivery systems.

## Processing and properties

The method by which RJS research has been conducted is all based on the same principle of a rotating spinneret (defined as an enclosed material container with multiple orifices) and some collection device – be that vertical collector bars, a solid cylindrical collector or a flat surface. In almost all cases, fibers were produced by altering the rotational velocity from 2,000 to 16,000 rpm, with some opting for higher rotational velocities due to smaller spinneret geometries where a similar centrifugal force would be required.

Altering the processing parameters in RJS yields a variation in fiber diameter. Processing variables within RJS include temperature, rotational velocity, collector distance, orifice diameter, and duration. Spin duration mainly affects the volume of the fibers yielded, but is nonetheless a basic parameter that is used in lab scale research. For continuous fiber production only the first group of variables needs to be considered. Other parameters that affect fiber properties and diameters will be related to the polymer material itself, depending on whether it is spun from solution or melt. Considering the material's spinnability, a certain upper (blockage) and lower (beading) limit for viscosity will exist for each combination of polymer solution concentration, or temperature for polymer melts.

Rotational velocity is what drives the process, and increasing this will yield a greater centrifugal force with which to eject the polymer from the orifice. This basic premise of RJS is utilized by Mellado et al. in their equation derived for the critical rotational velocity threshold as given below.<sup>169</sup>

$$\Omega_{th} = \sqrt{\frac{\sigma}{a^2 S_o \rho}} \quad (1)$$

Equation (1) signifies that for a given polymer, each threshold will differ based on measurements of stress ( $\sigma$ ), density ( $\rho$ ), orifice diameter ( $a$ ) and distance from centerline to orifice opening ( $S_o$ ). With these measurements obtained beforehand, the theory predicts that a critical rotational velocity should be selected for a chosen polymer melt/solution.

As mentioned, the viscoelasticity of the material affects the ability for a fiber to be spun. A study by Shanmuganathan et al. has shown the variance in fiber diameter of polybutylene

terephthalate (PBT) when altering the processing temperature.<sup>65</sup> Their data in Table 6 show that for a rotational speed of 12,000 rpm, the fiber diameter changed from 1.64  $\mu\text{m}$  at 280  $^{\circ}\text{C}$  to 1.17  $\mu\text{m}$  at 320  $^{\circ}\text{C}$ . This demonstrates that for PBT, an increase in processing temperature leads to thinner fibers. This will typically be the case for all polymers, as viscosity is reduced with temperature for thermoplastic polymers. It is worth noting that the viscosity of the polymer melt will have a great effect on spinnability, with low viscosity, Newtonian fluids being the best contenders as the standard systems are generally not pressure driven. For pressure driven systems see.<sup>153,170,171</sup>

Solution spinning does not rely on elevated temperatures as they are typically spun at room temperature. Instead of temperature, the reliance here will be on solution concentration and how it affects morphology of the fibers in the RJS process, as shown by Badrossamay et al. in Figure 12.

Their research demonstrates that jet break-up and therefore fiber quality may be estimated by the capillary number; defined as the ratio of the Weber number ( $We = \frac{\rho U^2 a}{\gamma}$ ) to the Reynolds number ( $Re = \frac{\rho U a}{\mu}$ ), which characterizes the ratio of the viscous force to surface tension force.  $\rho$  is density,  $\mu$  is dynamic viscosity (which is directly related to the molecular weight and solution concentration),  $\gamma$  is surface tension of the polymer solution,  $U$  is the polymer jet exit speed based on a stationary frame and  $a$  is the orifice diameter. A lower capillary number results in shorter jet lengths and earlier jet break-up to isolated droplets. It therefore highlights the critical polymer concentration for this polymer type, to produce the best quality polylactic acid (PLA) fibers.<sup>61</sup>

A study by Mohan et al.<sup>151</sup> has also investigated, in some detail, the ability of atactic-polystyrene (PS) to be melt spun by pressurized RJS. Here, the authors were particularly interested in molecular anisotropy of RJS fibers as compared to electrospun fibers with the highest level of anisotropy found in ES fibers. It was found that polymer solutions only yielded bead-free fibers between concentrations of 5–16 wt%. This type of range is a typical outcome for any study investigating the process conditions for bead-free fibers.

These types of analysis are a good methodology to employ for considering the types of polymers suitable for RJS, as this could potentially lead to further research whereby polymer properties can be used to approve or discard their ability to be spun without the time and effort expended on experimental testing.

## Fiber diameters

Fiber diameter measurements are a common and effective characterization method which is typically conducted using scanning electron microscopy (SEM),<sup>71,74,145</sup> optical microscopy (OM)<sup>65</sup> or transmission electron microscopy (TEM)<sup>172</sup> for imaging purposes.

The fiber diameters reported have several common influencing factors. Initial observations report a reduction in fiber diameter with an increase in rpm (therefore centrifugal force). In the case of PLA, an increase in the rotation speed from 4,000 to 12,000 rpm resulted in a reduction in fiber diameter from 1143 ( $\pm 50$ ) to 424 ( $\pm 41$ ) nm.<sup>61</sup> In the case of melt spinning, fiber diameters were also reduced with an increase in temperature

as previously noted, due to the reduction in melt viscosity with elevated temperatures. Zander<sup>76</sup> showed that with increasing PCL melt temperature, the fiber diameter initially decreased before increasing at an even lower viscosity due to high temperatures and potential polymer degradation (see Table 7).

A trend of a decreasing and then increasing fiber diameter was also shown for an increase in rotational velocity by O'Haire et al.<sup>74</sup> in which they attempted to melt spin fibers from a melt blowing grade polypropylene (Lyondell MF650Y, MFI = 1800 g dmin<sup>-1</sup>) and a 1 wt% concentration of MWCNT (multi-walled carbon nanotube) dispersion.

Reported in Table 8 is the proportion of fibers with a diameter greater than 5  $\mu\text{m}$ . This is a phenomenon that appears to show up in RJS as a by-product from the start of the spinning cycle. By producing nanofibers from a PCL solution, measurements taken by McEachin et al.<sup>63</sup> at different interval times (5, 10, 15, 30 s) throughout the spinning cycle demonstrated this issue (see Figure 10). Explaining this phenomenon, the authors describe the effect of droplet elongation in the initial stages of fiber drawing from the orifice, in which the initial fibers that are collected have not had time to fully elongate or have sufficient solvent evaporation yet. This leads to an equilibrium diameter being reached somewhere after around 30 s in the spinning cycle at 6,000 rpm (see Table 9). Due to this, many published mean fiber diameters from RJS will possibly have higher values due to the initial non-equilibrium state at start-up being included, and not accounted for.

O'Haire et al.<sup>74</sup> corrects for this start-up phenomenon by allowing fibers that fall into this initial spin duration to be discounted from the values of the averages quoted by setting a size limit of 5  $\mu\text{m}$ . Once these values are removed, a far more realistic mean value for the fiber diameter is obtained.

In research completed by Padron et al.,<sup>53</sup> the fiber spinning process was filmed at a high frame rate to view the polymer jet leaving the orifice (Figure 13). They investigated the effect of the angle of the orifice in comparison to the fiber diameters for a 6 wt% PEO solution at 6,000 rpm and concluded that the smallest diameter fiber was produced with a straight orifice, rather than 30 $^{\circ}$  in the direction of rotation, or 89 $^{\circ}$  against the direction of rotation.

Another influencing processing factor studied by Zander<sup>76</sup> illustrates the change in fiber diameter with collector distance variation. In his research, PCL fibers were collected at distances of 10, 12 and 14 cm from the orifice, producing fibers with diameters of  $8.2 \pm 5.8$ ,  $8.3 \pm 4.4$  and  $7.0 \pm 1.1$   $\mu\text{m}$ , respectively. Although this small amount of data is not conclusive, it does indicate that there is indeed a variation of fiber diameter with collector distance.

## Mechanical properties

Limited data are available in terms of mechanical properties of nanofibers produced by the RJS process, and nanofibers in general, due to the general difficulty in testing individual nanofibers. Nanoscale mechanical testing requires extremely small loads for deformation, along with expert handling of the fibers due to their size. According to Tan et al.,<sup>173</sup> the practicalities of testing individual nanofibers have the following five challenges: (1) Ability to manipulate extremely small fibers,



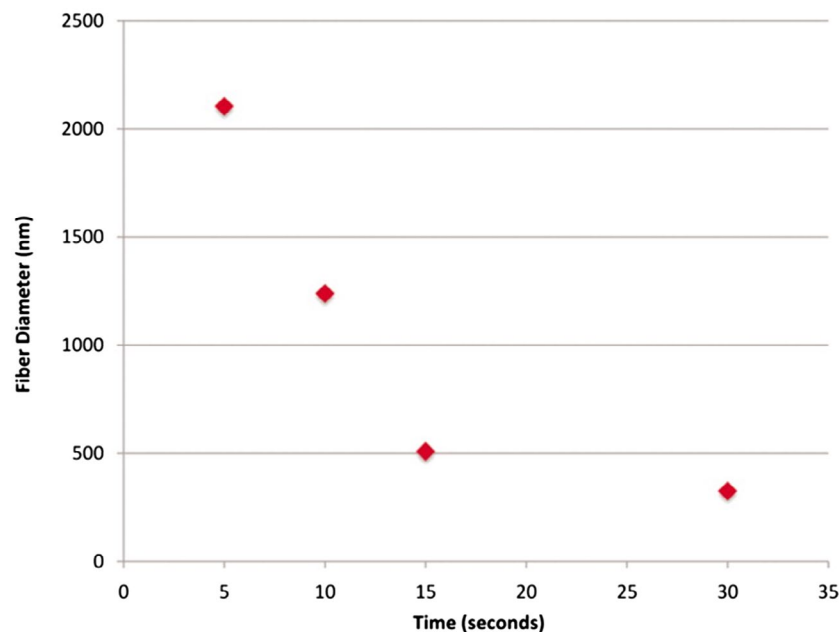


**Figure 10** Fiber diameter at various spinning times, showing a diameter reduction of RJS fibers during initial 30 s start up time, demonstrating the potentially skewed data of reported fiber diameter distributions if start up effects are not considered. Reprinted with permission from McEachin et al.,<sup>63</sup> Copyright 2012, John Wiley and Sons

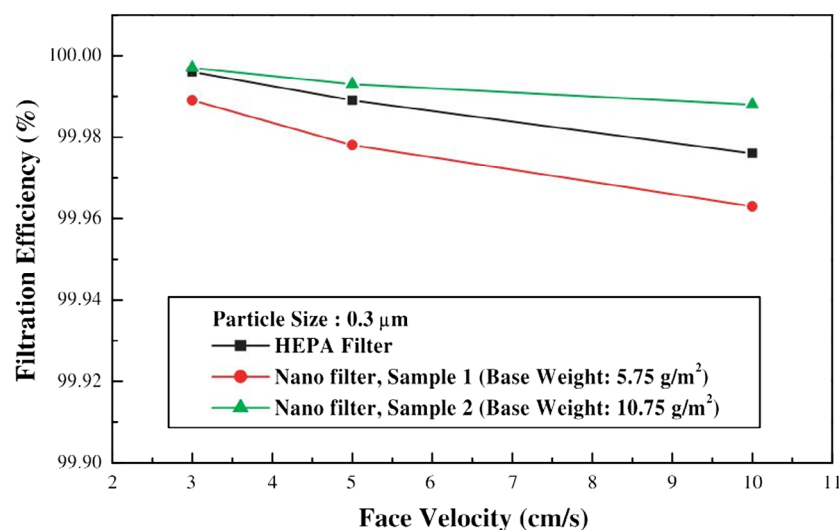


**Figure 11** Filtration efficiency of PA 6 nanofiber filters. Standard HEPA filter compared with two base weight nanofiber mats with average fiber diameters of 200 nm. Doubling the base weight led to a demonstrable increase in efficiency. Reprinted with permission from Ahn et al.,<sup>132</sup> Copyright 2006, Elsevier

(2) Finding a suitable mode of observation, (3) Sourcing of an accurate and sensitive force transducer, (4) Sourcing of an accurate actuator with high resolution, and (5) Preparing samples of single-strand nanofibers.

The most common methods of nanofiber tensile testing include the use of atomic force microscope (AFM) cantilevers,<sup>174–176</sup> 3-point bending testing<sup>177–179</sup> or commercial nano-tensile testing.<sup>38,127</sup> The AFM testing method essentially relies on the fixing of fibers to the ends of the AFM cantilever before applying a tensile load. Measuring the angle of deflection from the cantilever arm and fiber extension provides an

indication of the force required and therefore mechanical properties can be extrapolated.

In another method, Wang et al.<sup>177</sup> performed a 3-point bending test on electrospun PVA/MWCNT composite nanofibers to establish mechanical properties. They used an AFM cantilever to perform the test to measure fiber deflection, from which they could calculate the Young's modulus (Figure 14). These are however all time-consuming methods which require a high degree of precision, coupled with the fact that it remains difficult to manipulate single fibers within these test rigs.

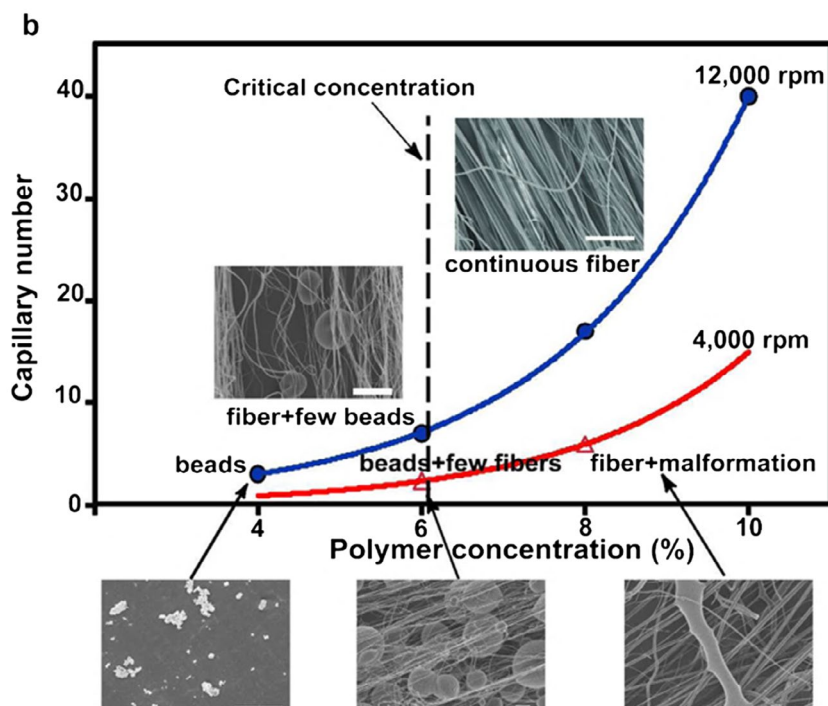


Figure 12 Nanofiber morphology reliance based on PLA concentration, showing that a critical concentration is needed to produce continuous bead-free fibers. Reprinted with permission from Badrossamay et al.,<sup>61</sup> Copyright 2010, American Chemical Society

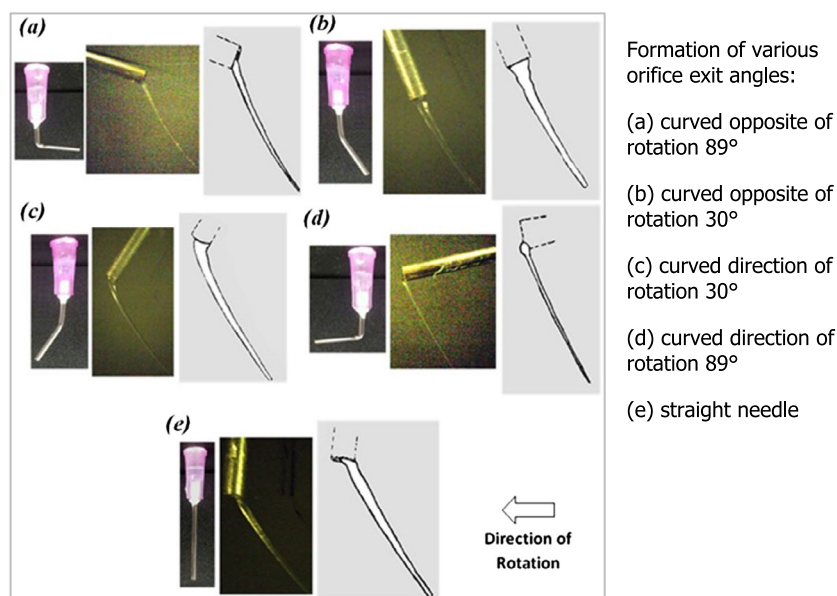


Figure 13 Analysis of the effect of orifice direction during spinning, showing that a straight needle (e) produced the smallest fiber diameter compared to other needle angles. Reprinted with permission from Padron et al.,<sup>53</sup> Copyright 2013, AIP Publishing LLC

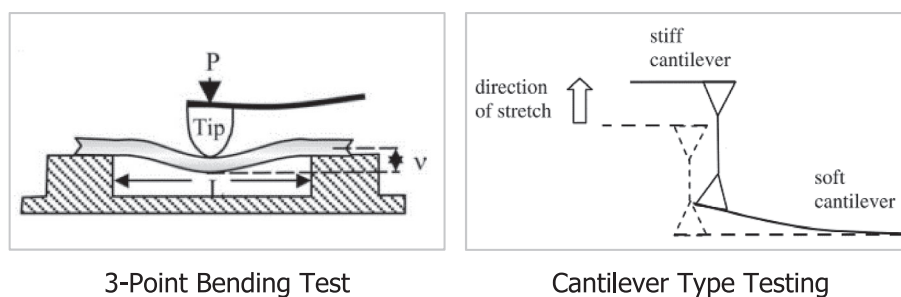
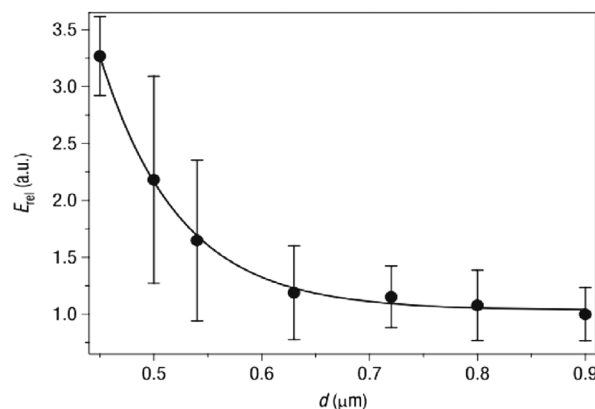


Figure 14 Methods of mechanical testing on nanofibers using AFM cantilevers. Reprinted with permission from Tan et al.,<sup>173</sup> Copyright 2006, Elsevier

Tensile testing using commercially available equipment can be conducted by collecting aligned fibers on a ready-made frame, for use in a universal tensile testing machine. Electrospun PCL and PLA nanofibers have been successfully tested in this way.<sup>180</sup> The single PCL fiber used in this experiment measured  $1.4 \pm 0.3 \mu\text{m}$ , with a tensile modulus of  $120 \pm 30 \text{ MPa}$  and a tensile strength of  $40 \pm 10 \text{ MPa}$  being observed. This publication also commented on the fact that there was no apparent correlation between Young's modulus



**Figure 15** Relative Young's modulus of PA 6,6 fibers as a function of diameter. These results show a definite increase in mechanical properties with reducing fiber diameters. Reprinted with permission from Arinstein et al.,<sup>181</sup> Copyright 2007, Nature Publishing Group

and fiber diameter in these fibers. Although fiber modulus generally increases with decreasing fiber diameter this effect is typically only observed for diameters below  $\sim 250 \text{ nm}$ ,<sup>126</sup> which is much lower than the  $1.4 \mu\text{m}$  of the fibers tested by Tan et al. Arinstein et al.,<sup>181</sup> for example, showed that a reduction in diameter of electrospun PA 6,6 fibers lead to a considerable increase in mechanical properties of these fiber due to improved molecular orientation and chain confinement (Figure 15).

Another option available in testing nanofibers is to test a bundle of multiple fibers together in a micro tensile tester. Yao et al.<sup>182</sup> tested electrospun co-polyimide nanofiber bundles of 30 nanofibers and reported a Young's modulus of 38 GPa and tensile strength of 1.6 GPa. The bundle data were evaluated using Daniels' theory<sup>183</sup> based on Weibull statistics in order to calculate individual fiber strengths.

Figure 16 shows the testing procedure of a single nanofiber using the framing method as proposed by Chen et al.<sup>184</sup> In their paper they discussed the mechanical properties of single electrospun polyimide nanofibers with a diameter of  $\sim 250 \text{ nm}$  and reported a record high tensile modulus of 89 GPa.

In the case of RJS, only a handful of publications have considered the mechanical properties of the materials produced. In one of these publications, Teflon nanofiber yarns were tested. The polymer solution was prepared by dissolving the Teflon in Fluorinert FC-40, before RJS and subsequently collecting and assembling as yarns. Tensile testing of these twisted yarns produced a modulus of 348 MPa.<sup>70</sup>

**Table 4** RJS (solution) materials choices from published data

Polymer	Application	Refs.
Poly(lactic acid) (PLA)	Biomedical, tissue engineering	[61]
Polyethylene oxide (PEO)		
Gelatine		
Poly(2,5-bis(20-ethyl-hexyl)-1,4-phenylenevinylene) (BEH-PPV)	Photo-luminescent qualities for applications in light emitting diodes	[64]
Polyethylene oxide (PEO)		
Polycaprolactone (PCL)	Study of RJS process	[63,144]
Polyvinylidene fluoride (PVDF)	Study of RJS process	[66]
Polytetrafluoroethylene (PTFE)	Super-hydrophobic properties for anti-fouling applications	[70]
Polyacrylonitrile (PAN)	Carbon fiber precursor	[67,145]
Poly(vinyl butyral) (PVB)	Study of RJS process	[84]
Polyvinylpyrrolidone (PVP)	Sacrificial polymer in fabrication of tin-doped indium oxide nanofibers	[62]
Polyvinylpyrrolidone (PVP)	Biomedical applications, drug delivery vehicle	[68,110]
Polycaprolactone (PCL)		
Poly(L-lactic acid) (PLLA)	Biomedical, tissue engineering	[71]
Polyvinylpyrrolidone (PVP)		
Polyvinylchloride (PVC)	Study of RJS process	[146]
Polyethylene glycol (PEG)		
Chitosan	Study of RJS process	[147,148]
Gelatine		
Polyurethane (PU)		
Polyamide 6 (PA6)		
Bacterial cellulose (BC)		
Polymethyl methacrylate (PMMA)		
Polyacrylonitrile (PAN)		
Polystyrene (PS)		
Polystyrene (PS)		
Polycarbomethylsilane (PCmS)		
Thermoplastic polyurethane (TPU)	Switchable hydrophobicity applications for oil-water separation, graphene composite filler study	[141,153]
Polyvinylpyrrolidone (PVP)		
SnCl <sub>4</sub> ·5H <sub>2</sub> O		
Polyvinyl alcohol (PVA)	Composite nanofiber for lithium-ion battery anodes	[155,156]
SnO <sub>2</sub> /PAN (Carbon)		
Polyvinylpyrrolidone (PVP)	Electrostatic-assisted RJS process	[157]

As mentioned earlier, so far RJS research has not been able to develop a deposition methodology that allows for fiber alignment in a similar way as the rotating drum or disc method does in electrospinning. By collecting oriented fibers,

**Table 5 RJS (melt) materials choices from published data**

Polymer	Application	Refs.
Polypropylene (PP)	Study of RJS process, Hydrophilic nonwoven applications	[69,74,140]
Polybutylene terephthalate (PBT)	Study of RJS process	[65]
Polycaprolactone (PCL)	Biomedical applications	[76,168]
Polyethylene terephthalate (PET)	Study of RJS process	[78]
Polyvinylpyrrolidone (PVP)		
Crystalline Olanzapine	Biomedical applications (Drug delivery)	[109]
Crystalline Piroxicam		
Crystalline Sucrose		

**Table 6 PBT fiber diameter variance with processing temperature, showing little variation with rotational velocity, but defined change from temperature affecting the polymer viscosity<sup>65</sup>**

Rotational speed (rpm)	Processing temperature (°C)	Average diameter (μm)	Std. deviation	% Nano-fibers
10,000	300	1.35	0.78	36
12,000	300	1.31	0.68	40
15,000	300	1.38	0.68	28
12,000	280	1.64	0.90	26
12,000	320	1.17	0.92	55

**Table 7 PCL fiber diameter with varying viscosity<sup>76</sup>**

Temperature (°C)	Viscosity (Pa s)	Fiber diameter (μm)
120	158.1	9.7 ± 4.9
140	130.4	8.8 ± 3.1
200	43.3	7.0 ± 1.1
250	17.8	12.8 ± 8.4

**Table 8 Melt processing effect on fiber diameter, showing the PP/MWCNT nanocomposite fiber variation in diameter with increasing spinneret speed<sup>74</sup>**

Compound	Spinneret speed (r min <sup>-1</sup> )	Mean fiber diameter (μm)	Proportion of fibers < 1 μm (%)	Mean fiber diameter (nm)	Proportion of fibers > 5 μm (%)
Pure PP	12,000	0.51	91.5	439	0
	13,000	0.63	88.3	502	0.7
PP/MWCNT	13,000	1.87	53.7	702	6.4
	14,000	1.05	56.7	633	0.6
	16,000	1.75	63.5	621	9.7

**Table 9 PCL fiber diameter variation with RJS time<sup>63</sup>**

Average fiber diameter of 16% PCL @ 6,000 rpm. Collected after 5, 10, 15, 30 s.		
Sample	Average diameter (nm)	Standard deviation (nm)
15% – 5 s	2105	±1004
16% – 10 s	1239	±895
16% – 15 s	509	±256
16% – 30 s	326	±112

it would ensure more accurate mechanical testing data using the frame method (see Figure 16). Upson et al. however used this method to test a nanofiber web produced by RJS, aligning the testing frame (and thereby the tensile testing direction) with the spinning direction of the fibers.<sup>164</sup>

Simplified methods of testing mechanical properties of polymer nanofibers are essential for future developments, although existing methods do provide some data which allows us to compare mechanical properties of nanofiber yarns,<sup>185</sup> bundles, and in rare occasions even single polymer nanofibers.

## Modeling the rotary jet spinning process

With any of the material's processing techniques available, modeling has a lot to offer to further refine and optimize the process. Knowledge that is gained from modeling is used to improve and understand the process in more detail, which is sometimes simply not possible through experimental techniques alone. Modeling the RJS process involves the use of basic parameters such as polymer viscosity, centrifugal force, Coriolis force, air drag on the fiber and also the evaporation time of a solvent in the collector during spinning.<sup>53</sup> Several publications investigating viscoelastic properties and production methods<sup>163,186–191</sup> provide great insight into the complexity of the RJS process, and will provide useful directions for future RJS models.

Models which focus on electrospinning have been published recently,<sup>49,192</sup> and these would naturally include additional properties such as the volumetric charge density and electrical potential during processing. One property which is obviously absent in electrospinning models are rotational velocities, but in many of these electrospinning models there is good agreement between predicted fiber morphology and that obtained through experimentation.

Figure 17 shows a basic representation of the forces involved in the RJS process in agreement with assumptions made by Mellado et al.<sup>169</sup>

There have been one-dimensional studies that have investigated related parameters such as spiraling slender jets emerging from a rapidly rotating orifice in both a viscous model by Decent



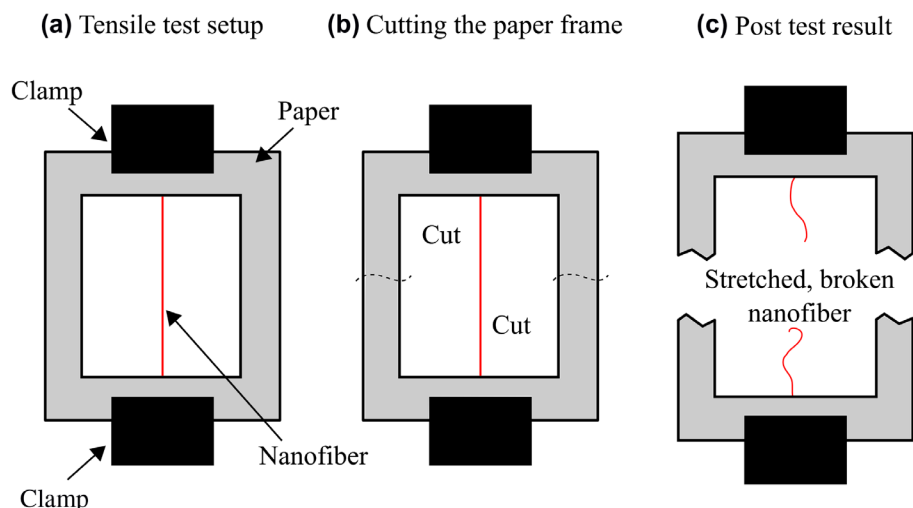


Figure 16 Tensile testing of a single polymer nanofiber using the paper frame method

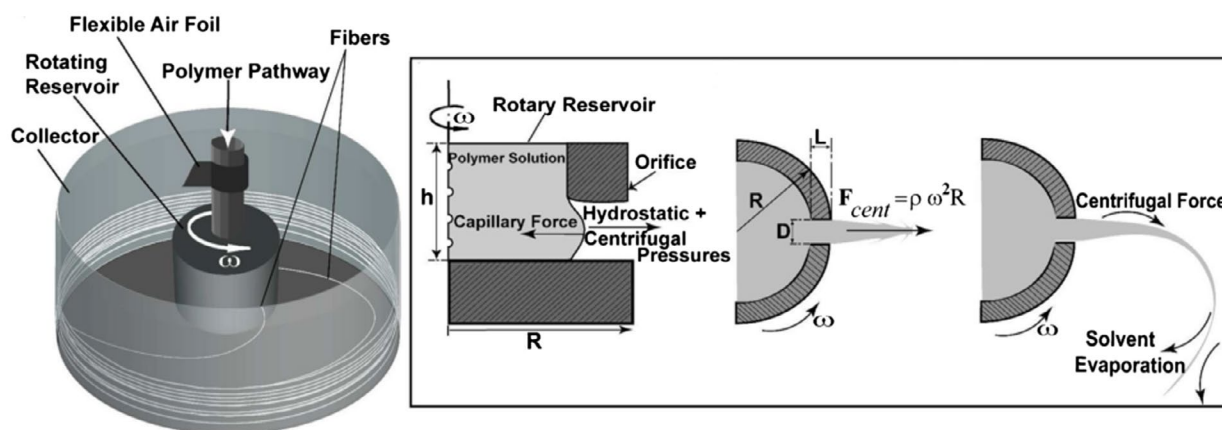


Figure 17 Schematic of RJS process with magnified views. Reprinted with permission from Badrossomay et al.,<sup>61</sup> Copyright 2010, American Chemical Society

et al.<sup>186</sup> and an inviscid model by Wallwork et al.<sup>193</sup> This research, and other related studies have set the initial basis for RJS models.

Valipouri et al.<sup>83,194</sup> performed experiments using both air-sealed (isolated) and open air (non-isolated) flow RJS setups to evaluate the prediction from a numerical model. The reason for this is due to the complexity of the addition of air resistance to the model once the system accounts for drag forces on the drawing fiber as it spins.

Based on coordinate systems from Wallwork et al.<sup>193</sup> and Decent et al.,<sup>186</sup> Valipouri et al.<sup>83</sup> established a model to evaluate the process. The main forces considered were centrifugal, Coriolis and viscous forces in a comparison between isolated and non-isolated models.

The model could accurately predict the experimental trajectory profiles for the isolated jets based on simulations (Figure 18), but was not able to accurately predict the trajectories of the non-isolated flow experiments, when using water as a test fluid.

The conclusion that Valipouri et al. reached was that an increase in trajectory curvature was found in the non-isolated open air system due to the increase in air resistance/turbulence within the spinning area. Fiber diameters of PAN were

also measured and compared with a simulation derived value, showing a correlation based on rotational velocity variation.

In a separate publication by Valipouri et al.<sup>194</sup> regarding the numerical study of RJS and the effect of angular velocity, they investigated the influence of non-dimensional numbers such as the Rossby number on fiber diameter. Here it was concluded that a decrease in Rossby number (which in real terms indicates an increase in angular velocity) reduces the size of the fiber diameter, contracts the trajectory, and increases the tangential velocity. This further enhances the experimental proof of reduced fiber diameter with increasing angular velocity, of which some qualitative agreement with experimental data has been established.

When investigating a new technique and possible ways to numerically evaluate its behavior, it may be possible to arrive at the same conclusions from different models, thus confirming each other's findings.

To this end, Mellado et al.<sup>169</sup> produced what they called "A simple model for nanofiber formation by rotary jet spinning". In it they establish three key moments in the lifecycle of nanofiber formation, namely (1) jet initiation, (2) jet elongation, and (3) solvent evaporation (Figure 19). It is in these three areas that experimental

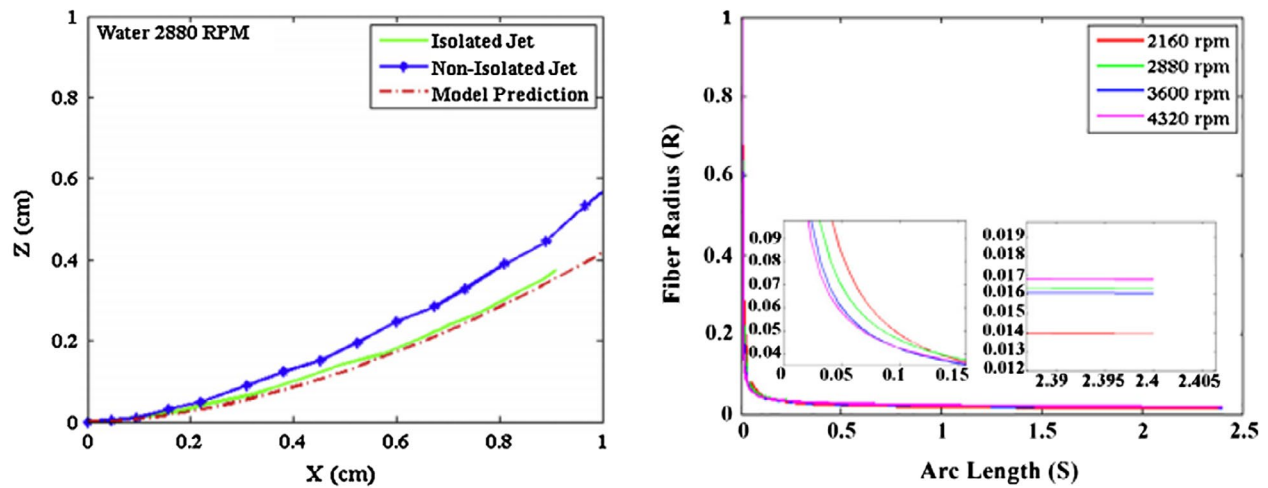


Figure 18 Experimental vs. model behavior of H<sub>2</sub>O (left) and polyacrylonitrile (PAN) (right). The model prediction of trajectory (left) shows the isolated jet and model having near identical values, whereas the real world non-isolated jet will experience air resistance, altering the trajectory which cannot be accounted for in the model. Fiber radius predictions (right) of PAN using a dimensionless value over the arc length show good correlation with measured experimental diameters, prediction only very small variances with speed. Reprinted with permission from Valipouri et al.,<sup>83</sup> Copyright 2015, Elsevier

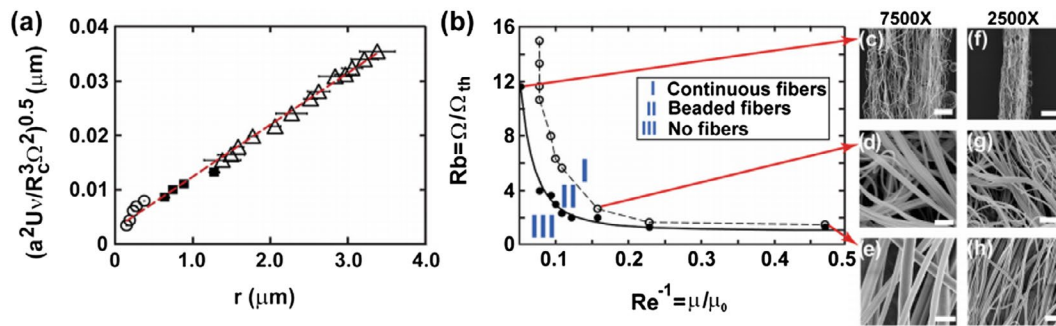


Figure 19 Phase diagram illustrating fiber prediction by Mellado et al.<sup>169</sup> showing: (a) Fiber radius measurements based around processing parameters (see publication for more details). (b) A phase diagram divides the scaled angular velocity-viscosity plane into regimes I, II, III. (c, f) Beady fibers. (d, g) Fine continuous fibers. (e, h) Large continuous fibers collected from regime I. Scale bars are 4 μm (c)–(e) and 20 μm (f)–(h). Reprinted with permission from Mellado et al. [169], Copyright 2011, AIP Publishing LLC

and theoretical studies produce a phase diagram, which can with some certainty predict the production rates and quality of fibers.

The final fiber radius and threshold rotational velocity for fiber production is calculated using the following equations, as proposed by Mellado et al.<sup>169</sup>:

$$r \sim \frac{aU^{0.5}v^{0.5}}{R_c^{3/2}\Omega} \quad (2)$$

where  $r$  is radius of fiber,  $a$  is orifice diameter,  $U$  is exit velocity of polymer,  $v$  is kinematic viscosity defined as viscosity/density,  $R_c$  is radius to collector and  $\Omega$  is rotational velocity.

$$\Omega_c \sim \frac{\rho R_c^2 \gamma^2}{a^2} \mu^{-3} \quad (3)$$

where  $\Omega_c$  is critical rotational velocity,  $\rho$  is density,  $R_c$  is radius to collector,  $\gamma$  is surface tension,  $a$  is orifice diameter and  $\mu$  is viscosity.

This study highlighted the fact that the formation of fibers using RJS is influenced by a few key factors. The tuning of fiber radii is essentially controlled by varying viscosity, angular velocity (which directly affects the polymer exit velocity), distance to

the collector and the radius of the orifice, which are all shown to be parameters in the model prediction for fiber radius.

While studying the interaction of the RJS process with various material property variations, Badrossamay et al.<sup>61</sup> experimented with polymer concentrations in solution as a benchmark for fiber quality. In their publication, they reviewed the effect of a change in polymer concentration on molecular chain entanglement, and the critical concentration at which the presence of a sufficient amount of entanglements dramatically alters the viscoelastic properties of the spinning solution to facilitate fibers of a higher quality (those without beading).

As with RJS, electrospinning also relies on chain entanglements. A detailed study by Shenoy et al.<sup>195</sup> has shown this to be the case for several polymer/solvent systems in which distinct zones are present, namely good fiber formation, fiber and bead formation, or beads or droplets only. In their research, Shenoy et al. calculated that for stable fiber formation to occur, a minimum of 2.5 entanglements per chain should exist.

A PVP/poly(L-lactic acid) (PLLA) and DCM solution was chosen to evaluate this phenomenon, with concentrations

ranging from 0.1 to 10%. In Figure 20, the gradient change of the zero shear viscosity versus polymer concentration signifies the alteration in molecular entanglements. There are usually three distinct regimes observed in these graphs, indicating a step change in the overlapping of polymer chains from a dilute, semi-dilute disentangled state to a semi-dilute entangled state. These gradients can vary depending on the different chain lengths, chain configurations, polydispersity and molecular weight of the PLLA and PVP in this study.<sup>71</sup>

It is typical in non-branched linear polymer melts for the zero shear viscosity to scale with the molecular weight to the power of  $\sim 3.4$  above the critical entanglement molecular weight,  $M_e$ ,<sup>196</sup> however polymer solutions can deviate from this gradient.<sup>197</sup>

It is this overlapping of polymer chains, with increase in polymer concentration, which results in a critical concentration being reached. In the case of RJS of PLA/chloroform, this is in the region of 8 wt%. At this concentration, there are enough chain entanglements to create a viscoelastic solution that can produce bead-free fibers at sufficient rotational velocities. As shown in Figure 12, the critical concentration may indicate when a polymer solution is likely to produce a good quality fiber, but the angular velocity must still be sufficient to overcome the surface tension in the drawn fiber so as not to induce malformations such as beading.

As with previous modeling examples in RJS, non-dimensional numbers are often the key to understanding the limitations of the process. In Badrossamay's evaluation of them,<sup>61</sup> the Capillary number (defined as the ratio of the Weber number to the Reynolds number) indicates whether a fiber would be of better quality by possessing a higher value. They state that the Capillary number could estimate jet break-up, whereby lower Capillary numbers result in shorter jet lengths and earlier jet break-up to isolated droplets.<sup>61,198</sup>

The two-dimensional (2D) inviscid model for RJS focuses on determining the fiber radius and trajectories as a function of arc length and was produced by Pardon et al.<sup>199</sup> This model is geared toward predicting final fiber diameters, with the hope of reducing experimental time and material waste. To do this,

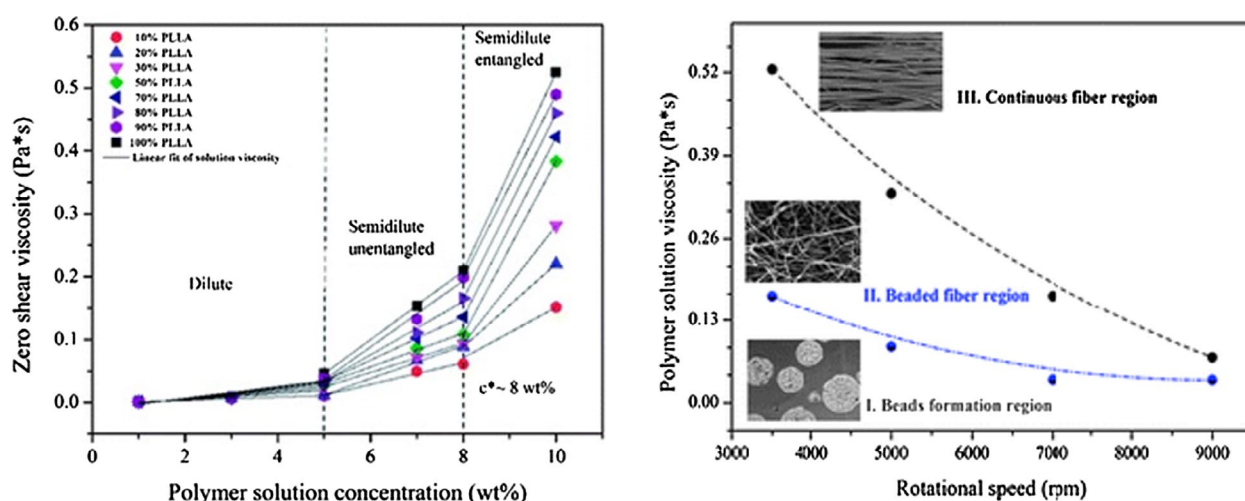
the parameters studied included angular velocity, material properties, collector diameter, orifice size and solvent evaporation rate. This model is however 2D which assumes that the gravitational forces are much smaller than the centrifugal forces produced in the system.

Non-dimensional numbers provide ratios between various forces in the system being studied. Padron et al.<sup>64</sup> reviews some of the most important ones in Table 10.

Padron et al. produced comparable solutions to those of Wallwork et al.<sup>193</sup> where the trajectory and diameters of beads formed using the prilling process are studied. This process is similar to RJS and based on viscous material ejected from a rotating surface, typically used to create pellets from materials heated to low viscosity melting points such as fertilizers or detergent powders.<sup>200</sup> The steady state solutions that were obtained were then used to compare similarly derived equations for time-dependant parameters with constant angular velocity, transforming the equations into partial differential equations.

Padron et al.'s work clearly displays an ability to model and predict the variation in fiber diameter along its axis with respect to time, including information on the trajectory of such fibers. However, their work does not include a viscous element, and could therefore be misleading when comparing with experimental data. However, with a viscoelastic component included in such a model, a powerful prediction tool would become available.

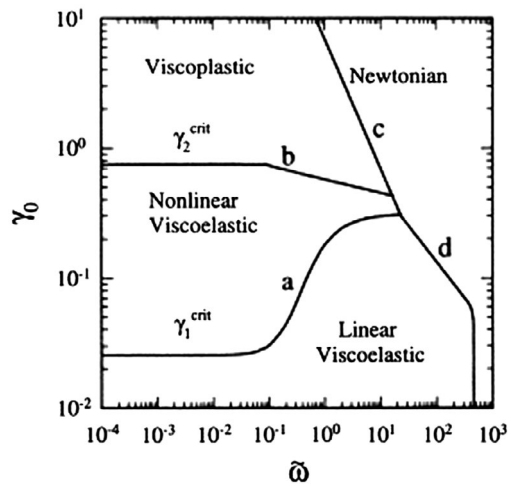
Such a model was presented in a further publication by Padron et al.<sup>53</sup> in which they study the fiber forming process from a material property point of view, along with high speed photography to capture the physics of the jet as it leaves the orifice. This work once again summarized the importance of all of the processing parameters including viscoelastic properties, viscosity and relaxation time of the polymeric material. As discussed by Padron et al.,<sup>53</sup> it is important to consider the large deformations that are present in the RJS process, and to choose appropriate viscoelastic models which will be able to approximate the solution or material properties such as a Pipkin diagram,<sup>201</sup> which separates a materials' viscoelastic



**Figure 20** Zero shear viscosity versus polymer solution concentration for polyvinylpyrrolidone/poly(L-lactic acid) (PVP/PLLA) blends with varying PLLA content (left) and PVP/PLLA fiber quality (right), showing how the critical entanglement ratio affects the quality of the fiber throughout all spinning speeds. Reprinted with permission from Ren et al.,<sup>71</sup> Copyright 2013, Royal Society of Chemistry

**Table 10** Non-dimensional numbers used for prediction of fluid behavior. Adapted from Padron et al.<sup>64</sup>

Dimensionless number	Ratio description
Reynolds number	Inertial forces to viscous forces
Froude number	Fibre's inertial force to gravitational force
Weber number	Fibre's inertial force to surface tension
Rossby number	Fibre's inertial force to Coriolis force
Deborah number	Polymer relaxation time to flow
Capillary number	Fibre's viscous forces to surface tension


**Figure 21** Pipkin diagram showing demarcated areas of viscoelastic behavior, evaluating strain amplitude ( $\gamma_0$ ) versus dimensionless frequency ( $\omega$ ). Reprinted with permission from Parthasarathy et al.,<sup>202</sup> Copyright 1999, Elsevier

properties into regimes based on their dynamic response (Figure 21).

In their research, Padron et al. define RJS falling into the non-linear viscoelastic regime in Figure 21. It goes on to define the coordinate system using a rotating reference, and the governing equations used are described by the continuity equation:

$$\nabla \cdot \mathbf{U} = 0 \quad (4)$$

where  $\mathbf{u}$  is the relative velocity of the fiber jet.

And the Cauchy momentum equations:

$$\frac{\partial \mathbf{U}}{\partial t} + (\mathbf{U} \cdot \nabla) \mathbf{U} = -\frac{\nabla P}{\rho} + \mathbf{g} + \frac{\nabla \mathbf{T}}{\rho} - \Omega(\Omega \mathbf{c}) - 2\Omega \mathbf{U} \quad (5)$$

where  $P$  is the pressure,  $\mathbf{g}$  is the gravity vector,  $\mathbf{T}$  is the stress tensor,  $\Omega$  is the angular velocity of the spinneret, and  $\mathbf{c}$  is a position vector describing a point along the fiber.

Exit velocities for both continuous and non-continuously fed spinnerets are calculated using the parameters from Figure 22.

Based on these calculations for velocity  $U$ , the critical angular velocity  $\Omega_{cr}$  and critical exit velocity  $U_{cr}$  of the system were established.

$$\Omega_{cr} = \sqrt{\frac{2\pi \frac{a}{2} \mu \sin \alpha}{\rho V_{pd} S_0}} \quad (6)$$

where  $\rho$  is density,  $V_{pd}$  is volume of the pendant drop.

$$U_{cr} = -\frac{8L\mu}{\rho \left(\frac{a}{2}\right)^2} \frac{1}{2} \sqrt{256 \left(\frac{L\mu}{\rho \left(\frac{a}{2}\right)^2}\right)^2 \frac{8\pi \left(\frac{a}{2}\right) \mu \sin \alpha}{\rho V_{pd} S_0} \left[R_c^2 2L \left(S_0 - \frac{L}{2}\right)\right]} \quad (7)$$

High speed imagery was used to establish the shape of the pendant drop as it approaches the critical velocity threshold, which results in fiber jet initiation. After this point, when the fiber has commenced its extension, the velocity of the jet increases due to the simultaneous pushing and pulling momentum from both sides of the capillary (Figure 23). This velocity is expressed in an equation by Padron et al.<sup>53</sup> by adding an additional term  $U_f$  (fiber velocity) into the above velocity equation.

Padron et al.<sup>53</sup> also experimented by varying both angular velocities and solution viscosity, and were able to establish a model of trajectories along the  $X$  and  $Z$  axis as seen in Figure 24.

Being able to accurately predict the final radius and trajectory for the RJS process is important in the long term as industrial applications for nanofibers become more refined. When the basic morphology can be predicted to a reasonably acceptable accuracy, the process becomes more commercially viable. The current data available to achieve this are approaching the point to which this would be possible.

## Adaptations within rotary jet spinning

As RJS is still a relatively new technique for manufacturing polymer nanofibers, there are different approaches in the design and construction of the equipment used. These variations are often based on a few key parameters which alter the spinneret size, collector distance and rotational velocity, with some changing the number of jet orifices and locations. According to the centrifugal force equation ( $F_c = M\omega^2 r$ ), an equivalent force can be obtained by either altering the rotational velocity or by altering the distance from the axes of rotation – with the rotational velocity being the more sensitive parameter.

Commercial versions of RJS hardware are available to purchase from companies such as FibeRio<sup>®</sup> Technology Co. in Texas, USA, and around a third of publications have used their flagship Cyclone<sup>™</sup> spinner to conduct research into nanofiber production. Current availability is unknown since acquisition by CLARCOR in 2016, which in turn were acquired by Parker Hannifin in 2017. Alternatively, an extremely simple setup could involve nothing more than an inverted motor with a polymer vessel acting as a spinneret, surrounded by a collection device. In essence, a very simple setup – not very different from a candy floss machine – should you wish to conduct research on varying dimensional scales other than that which is available commercially. However, accuracy and repeatability would rely on the quality of equipment being used with safety being another key consideration.

Other adaptations of the process by which to make fibers through centrifugal force have involved experiments using nozzle-free approaches, such as the one used by Weitz et al.<sup>203</sup> in their study of poly(methyl methacrylate) (PMMA) solution



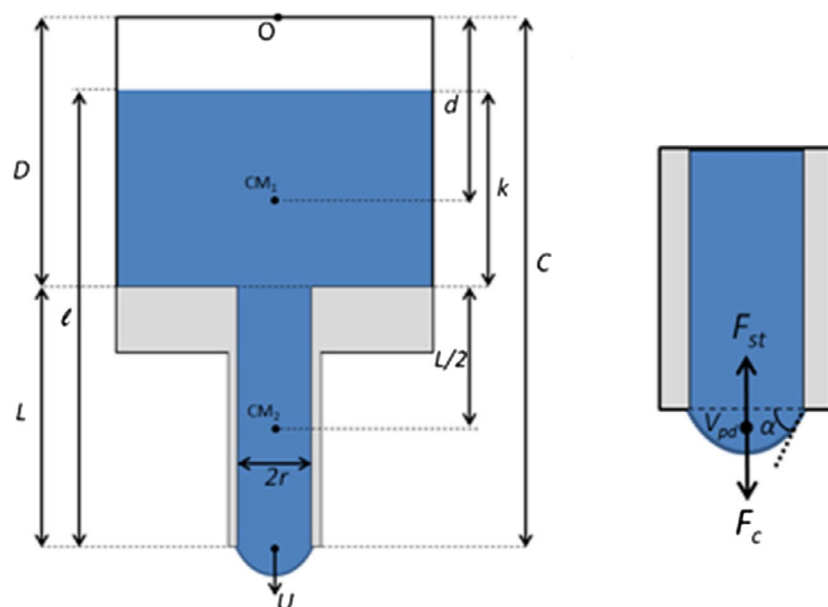


**Figure 22** Forces on material with spinneret and pendant drop. Reprinted with permission from Padron et al.,<sup>53</sup> Copyright 2013, AIP Publishing LLC

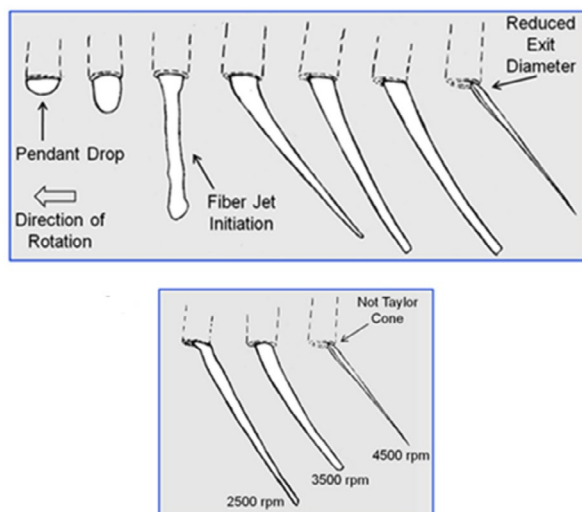


**Figure 23** Evolution of jet at orifice for fiber production as it accelerates to 4,500 rpm, with additional jet shapes for varying speeds. This shows the changeover from pendant drop to full fiber producing flow. Reprinted with permission from Padron et al.,<sup>53</sup> Copyright 2013, AIP Publishing LLC

behavior on the surface of a spin coater. They were interested in this technique and established a procedure to create discontinuous fibers in the diameter range of 25 nm to 5  $\mu$ m.

Methods that incorporate electrospinning together with an element of RJS have also been investigated. Angammana et al.<sup>204</sup> considered a charged rotary atomiser disc with polymer solution that would effectively eject fibers from the top of the rotational arc toward a charged collector plate above, resulting in nanofiber production. A similar technique was introduced by Chang et al.<sup>205</sup> They combined electrospinning with RJS and termed it electrostatic-centrifugal spinning, with the view of removing the whipping instability experienced by electrospinning alone. It is said to be first introduced by their lab, and

they investigated the effects on a viscoelastic jet and a single nanofiber through this technique. Much emphasis was placed on the viscoelastic behavior of the jets. Badrossomay et al.,<sup>128</sup> Ericksson et al.<sup>129</sup> and Wang et al.<sup>110</sup> have also produced good fiber alignment by combining both RJS and electrospinning.

The benefit of this process is to ensure that fiber alignment is maximized. If the fiber is moving toward the collector in electrospinning, a whipping motion is experienced, creating a non-oriented mat on the collector. By introducing RJS to this process, it greatly increases alignment, much in the same way that a rotating disc collector in electrospinning ensures fiber alignment on collection.

Pressure can also be used as an added element to improve RJS. If the spinneret is enclosed and pressurized, an additional force is introduced. This is exactly what Edirisinghe and co-workers did when spinning several materials from solution under a pressure of up to 300 kPa and 36,000 rpm, being the capability of their in-house built system.<sup>153,165,168,170,171,206–210</sup> The benefits of this system include the use of a wider range of polymer viscosities due to added pressure forcing flow through the spinneret dies, rather than relying purely on centrifugal force generated by the rotation velocity. This system does not however seem to produce fibers consistently in the nanoscale.

## The future of rotary jet spinning

Rotary jet spinning has become prevalent in the last decade, with research related to this topic increasing exponentially since its inception. At present, the commercialization of this technology for the nonwoven industry is starting, with the introduction of larger industrial scale RJS machines capable of spinning one meter wide continuous fiber mats. Other methods of nanofiber production such as needleless electrospinning also offer large scale production, such as the Nanospider™ technology by Elmarco,<sup>7</sup> as referenced previously. However, with up-scaled nanofiber production, it is only a matter of time

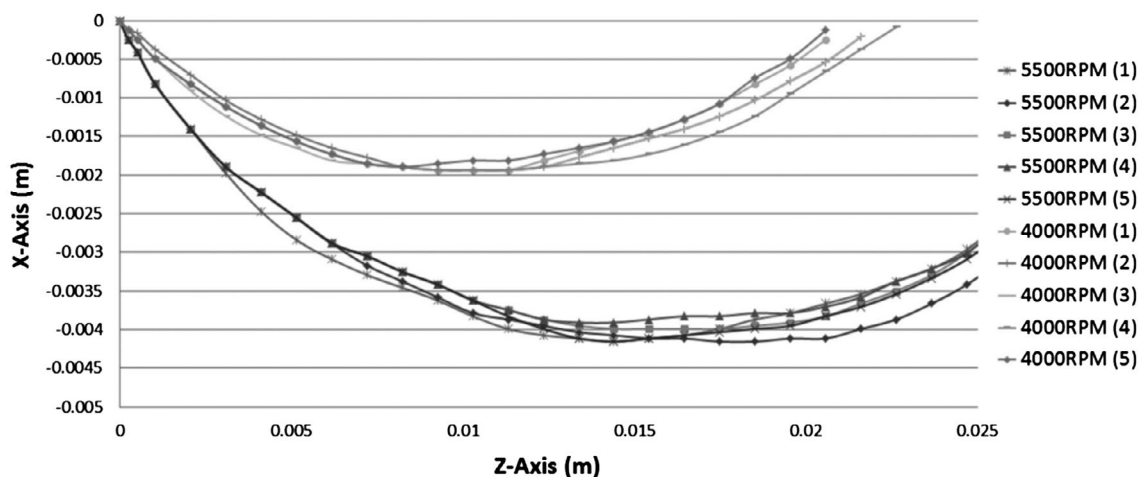


**Figure 24** Variance of fiber trajectories under same conditions, showing effect of viscosity on fiber trajectory. 6 wt% PEO solutions were used at two velocities in order to obtain trajectory data. The higher rotational velocities ensured a tighter trajectory compared with slower velocities. Reprinted with permission from Padron et al.,<sup>53</sup> Copyright 2013, AIP Publishing LLC

until RJS starts to compete with other more established methods of polymer nanofiber production such as melt blowing, where unaligned non-woven mats and spunbound materials are made.

Due to the lower production costs and potentially greener credentials, a lower price to market should be achievable which could make this a potentially disruptive technology in the nanofiber race. However, it remains to be seen whether a broad range of materials will be considered for diverse applications, or if more traditional polymeric materials such as polypropylenes, polyamides or polyesters will take on specific product applications. Since biomedicine is a large contributor to the research bulk to date, it is possible that pharmaceutical/ biomedical interests may become the lead user of this technology for the development of tissue recovery and/or drug delivery systems. Other applications at the forefront of this technology will be in fiber-based electronic devices like flexible sensors, super capacitors or lithium ion batteries.

As with most technology, the more that is understood about the ability to manipulate a certain production method, the more attractive it is for investment within them. The current body of knowledge available on RJS would suggest that we can expect a step change to occur well within the next decade.

## Funding

The authors gratefully acknowledge DSM (the Netherlands) for financial support and actively supporting our research in the field of RJS.

## Disclosure statement

No potential conflict of interest was reported by the authors.

## References

- 1 A. L. Yarin, B. Pourdeyhi and S. Ramakrishna: 'Fundamentals and applications of micro and nanofibers', 2014, Cambridge, Cambridge University Press.
- 2 N. Bhardwaj and S. C. Kundu: 'Electrospinning: a fascinating fiber fabrication technique', *Biotechnol. Adv.*, **2010**, *28*, (3), 325–347.
- 3 K. Graham, M. Ouyang, T. Raether, T. Grafe, B. McDonald and P. Knauf: 'Polymeric nanofibers in air filtration applications' In: Fifteenth Annual Technical Conference & Expo of the American Filtration & Separations Society, Galveston, Texas, 2002 Apr 9, pp. 9–12.
- 4 D. R. Paul and L. M. Robeson: 'Polymer nanotechnology: Nanocomposites', *Polymer*, **2008**, 3187–3204.
- 5 M. H. G. Wichmann, K. Schulte and H. D. Wagner: 'On nanocomposite toughness', *Compos. Sci. Technol.*, **2008**, *68*, (1), 329–331.
- 6 I. Greenfeld and H. D. Wagner: 'Nanocomposite toughness, strength and stiffness: Role of filler geometry', *Nanocomposites*, **2015**, *1*, (1), 3–17.
- 7 Elmarco.com, 'Elmarco – Nano for Life', 2015, available at <http://www.elmarco.com/gallery/nanofibers/>, (accessed 8 September 2015).
- 8 J. Yao, C. Bastiaansen and T. Peijs: 'High strength and high modulus electrospun nanofibers', *Fibers*, **2014**, *2*, (2), 158–186.
- 9 Z.-M. Huang, Y. Z. Zhang, M. Kotaki and S. Ramakrishna: 'A review on polymer nanofibers by electrospinning and their applications in nanocomposites', *Compos Sci Technol*, **2003**, *63*, (15), 2223–2253.
- 10 A. Greiner and J. H. Wendorff: 'Electrospinning: a fascinating method for the preparation of ultrathin fibers', *Angew. Chem. Int. Ed. Engl.*, **2007**, *46*, (30), 5670–5703.
- 11 R. L. Shambaugh: 'A macroscopic view of the melt-blowing process for producing microfibers', *Ind. Eng. Chem. Res.*, **1988**, *27*, (12), 2363–2372.
- 12 W. Han, G. S. Bhat and X. Wang: 'Investigation of nanofiber breakup in the melt-blowing process', *Ind. Eng. Chem. Res.*, **2016**, *55*, (11), 3150–3156.
- 13 A. Durany, N. Anantharamaiah and B. Pourdeyhi: 'High surface area nonwovens via fibrillating spunbonded nonwovens comprising islands-in-the-sea bicomponent filaments: structure–process–property relationships', *J. Mater. Sci.*, **2009**, *44*, (21), 5926–5934.
- 14 N. Anantharamaiah, S. Verenich and B. Pourdeyhi: 'Durable nonwoven fabrics via fracturing bicomponent islands-in-the-sea filaments', *J. Eng. Fibers Fabr.*, **2016**, *3*, (3), 1–9.
- 15 Z. Zhang, W. Tu, T. Peijs and C. W. M. Bastiaansen: 'Fabrication and properties of poly(tetrafluoroethylene) nanofibers via sea-island spinning', *Polymer*, **2017**, *109*, 321–331.
- 16 C. Schönenberger, B. M. I. van der Zande, L. G. J. Fokkink, M. Henny, C. Schmid, M. M. Krüger, A. Bachtold, R. A. Huber, H. Birk and U. Staufer: 'Template synthesis of nanowires in porous polycarbonate membranes: electrochemistry and morphology', *J. Phys. Chem. B*, **1997**, *101*, (28), 5497–5505.
- 17 K. Lozano and S. Kamalaksha: 'Superfine fiber creating spinneret and uses thereof', U.S. Patent No. 8,231,378. 31 Jul. 2012.
- 18 X. Zhang and Y. Lu: 'Centrifugal spinning: an alternative approach to fabricate nanofibers at high speed and low cost', *Polym. Rev.*, **2014**, *54*, (4), 677–701.
- 19 E. Peno and R. Lipton: 'Apparatuses and methods for the simultaneous production of microfibers and nanofibers', U.S. Patent No. 8,647,541 B2. 11 Feb. 2014.

- 20 E. Peno and R. Lipton: 'Devices and methods for the production of coaxial microfibers and nanofibers', U.S. Patent No. 8,709,309 B2. 29 Apr. 2014.
- 21 E. Peno and R. Lipton and S. Kay: 'Apparatuses having outlet elements and methods for the production of microfibers and nanofibers', U.S. Patent No. 8,647,540 B2. 11 Feb. 2014.
- 22 E. Peno and R. Lipton and S. Kay: 'Apparatuses and methods for the deposition of microfibers and nanofibers on a substrate', U.S. Patent No. 8,658,067 B2. 25 Feb. 2014.
- 23 E. Peno and R. Lipton and S. Kay: 'Multilayer apparatuses and methods for the production of microfibers and nanofibers', U.S. Patent No. 8,777,599 B2. 15 Jul. 2014.
- 24 E. Peno and R. Lipton and S. Kay: 'Split fiber producing devices and methods for the production of microfibers and nanofibers', U.S. Patent No. 8,778,240 B2. 15 Jul. 2014.
- 25 E. Peno and R. Lipton and S. Kay: 'Systems and methods for the production of microfibers and nanofibers using a fluid level sensor', U.S. Patent No. 8,858,845 B2. 14 Oct. 2014.
- 26 European Patent Office, available at <http://www.epo.org/>, (accessed 23 September 2015).
- 27 T. Ondarçuhu and C. Joachim: 'Drawing a single nanofibre over hundreds of microns', *Europhys Lett.*, **1998**, **42**, (2), 215–220.
- 28 P. B. McDaniel, J. M. Deitzel and J. W. Gillespie: 'Structural hierarchy and surface morphology of highly drawn ultra high molecular weight polyethylene fibers studied by atomic force microscopy and wide angle X-ray diffraction', *Polymer*, **2015**, **29**, 148–158.
- 29 L. Feng, S. Li, H. Li, J. Zhai, Y. Song, L. Jiang and D. Zhu: 'Superhydrophobic surface of aligned polyacrylonitrile nanofibers', *Angew. Chem. Int. Ed. Engl.*, **2002**, **41**, (7), 1221–1223.
- 30 J. Wang and D. Zhang: 'One-dimensional nanostructured polyaniline: syntheses, morphology controlling, formation mechanisms, new features, and applications', *Adv. Polym. Technol.*, **2013**, **32**, (S1), E323–E368.
- 31 P. X. Ma and R. Zhang: 'Synthetic nano-scale fibrous extracellular matrix', *J. Biomed. Mater. Res.*, **1999**, **46**, (1), 60–72.
- 32 G. M. Whitesides and B. Grzybowski: 'Self-assembly at all scales', *Science*, **2002**, **295**, (5564), 2418–2421.
- 33 J. D. Hartgerink, E. Beniash and S. I. Stupp: 'Self-assembly and mineralization of peptide-amphiphile nanofibers', *Science*, **2001**, **294**, (5547), 1684–1688.
- 34 S. Zhang: 'Fabrication of novel biomaterials through molecular self-assembly', *Nat. Biotechnol.*, **2003**, **21**, (10), 1171–1178.
- 35 N. Fedorova and B. Pourdeyhimi: 'High strength nylon micro- and nanofiber based nonwovens via spunbonding', *J. Appl. Polym. Sci.*, **2007**, **104**, (5), 3434–3442.
- 36 W. J. Li, C. T. Laurencin, E. J. Caterson, R. S. Tuan and F. K. Ko: 'Electrospun nanofibrous structure: A novel scaffold for tissue engineering', *J. Biomed. Mater. Res.*, **2002**, **60**, (4), 613–621.
- 37 T. M. Araujo, S. Sinha-Ray, A. Pegoretti and A. L. Yarin: 'Electrospinning of a blend of a liquid crystalline polymer with poly(ethylene oxide): Vectran nanofiber mats and their mechanical properties', *J. Mater. Chem. C*, **2013**, **1**, (2), 351–358.
- 38 J. Yao, J. Jin, E. Lepore, N. M. Pugno, C. W. M. Bastiaansen and T. Peijs: 'Electrospinning of p-Aramid Fibers', *Macromol. Mater. Eng.*, **2015**, **300**, 1238–1245.
- 39 M. Bognitzki, W. Czado, T. Frese, A. Schaper, M. Hellwig, M. Steinhart, A. Greiner and J. H. Wendorff: 'Nanostructured fibers via electrospinning', *Adv. Mater.*, **2001**, **13**, (1), 70–72.
- 40 D. Li and Y. Xia: 'Fabrication of titania nanofibers by electrospinning', *Nano Lett.*, **2003**, **3**, (4), 555–560.
- 41 H. Yoshimoto, Y. M. Shin, H. Terai and J. P. Vacanti: 'A biodegradable nanofiber scaffold by electrospinning and its potential for bone tissue engineering', *Biomaterials*, **2003**, **24**, (12), 2077–2082.
- 42 C. J. Ellison, A. Phatak, D. W. Giles, C. W. Macosko and F. S. Bates: 'Melt blown nanofibers: Fiber diameter distributions and onset of fiber breakup', *Polymer*, **2007**, **48**, (11), 3306–3316.
- 43 M. J. Moreno, A. A. Ajji, D. Mohebbi-Kalhari, M. P. Rukhlova, A. Hadjizadeh and M. N. Bureau: 'Development of a compliant and cytocompatible micro-fibrous polyethylene terephthalate vascular scaffold', *J. Biomed. Mater. Res. B: Appl. Biomater.*, **2011**, **97B**, (2), 201–214.
- 44 R. R. Breese and W.-C. Ko: 'Fiber formation during melt blowing', *Int. Nonwovens J.*, **2003**, **12**, (2), 21–28.
- 45 R. Nayak, R. Padhye, I. L. Kyratzis, Y. B. Truong and L. Arnold: 'Recent advances in nanofibre fabrication techniques', *Text. Res. J.*, **2011**, **82**, 129–147.
- 46 H. Zhou, T. B. Green and Y. L. Joo: 'The thermal effects on electrospinning of polylactic acid melts', *Polymer*, **2006**, **47**, (21), 7497–7505.
- 47 M. Yu, R.-H. Dong, X. Yan, G.-F. Yu, M.-H. You, X. Ning and Y.-Z. Long: 'Recent advances in needleless electrospinning of ultrathin fibers: From academia to industrial production', *Macromol. Mater. Eng.*, **2017**, **302**, (7), 1700002.
- 48 T. D. Brown, P. D. Dalton and D. W. Huttmacher: 'Melt electrospinning today: an opportune time for an emerging polymer process', *Prog. Polym. Sci.*, **2016**, **56**, 116–166.
- 49 R. R. Stepanyan, A. V. Subbotin, L. Cuperus, P. Boonen, M. Dorschu, F. Oosterlinck and M. J. H. Bulters: 'Nanofiber diameter in electrospinning of polymer solutions: Model and experiment', *Polymer*, **2016**, **97**, 428–439.
- 50 C. J. Luo, S. D. Stoyanov, E. P. J. Stride, E. G. Pelan and M. J. Edirisinghe: 'Electrospinning versus fibre production methods: From specifics to technological convergence', *Chem. Soc. Rev.*, **2012**, **41**, (13), 4708–4735.
- 51 G. C. Rutledge and S. V. Fridrikh: 'Formation of fibers by electrospinning', *Adv. Drug Deliv. Rev.*, **2007**, **59**, (14), 1384–1391.
- 52 W. K. Son, J. H. Youk, T. S. Lee and W. H. Park: 'The effects of solution properties and polyelectrolyte on electrospinning of ultrafine poly(ethylene oxide) fibers', *Polymer*, **2004**, **45**, (9), 2959–2966.
- 53 S. Padron, A. Fuentes, D. Caruntu and K. Lozano: 'Experimental study of nanofiber production through forspinning', *J. Appl. Phys.*, **2013**, **113**, (2), 9.
- 54 N. Hiremath and G. S. Bhat: 'Meltblown polymeric nanofibres for medical applications – an overview', *Nanosci. Technol.*, **2015**, **2**, (1), 1–9.
- 55 D. Wang, G. Sun and B.-S. Chio: 'A high-throughput, controllable, and environmentally benign fabrication process of thermoplastic nanofibers', *Macromol. Mater. Eng.*, **2007**, **292**, (4), 407–414.
- 56 Fiber Engine FX series systems from FibeRio, 2014, available at <http://www.filtsep.com/view/40670/fiber-engine-fx-series-systems-from-fiberio/>, (accessed 29 June 2017).
- 57 Nanofiber production line NS 851600U, 2017, available at <http://www.elmarco.com/nanofiber-equipment/nanofiber-production-lines-ns851600u/>, (accessed 29 June 2017).
- 58 Equipment NW-101 MECC CO. Ltd, 2017, available at <http://www.mecc-nano.com/equipment01.html>, (accessed 29 June 2017).
- 59 Industrial electrospinning nanofiber machine | Inovenso, innovative engineering solutions, 2017, available at <http://inovenso.com/portfolio-view/nanospinner416/>, (accessed 29 June 2017).
- 60 SPIN Line by SPUR, 2017, available at <http://www.spur-nanotechnologies.cz/>, (accessed 29 June 2017).
- 61 M. R. Badrossamay, H. A. McIlwee, J. A. Goss and K. K. Parker: 'Nanofiber assembly by rotary jet-spinning', *Nano Lett.*, **2010**, **10**, (6), 2257–2261.
- 62 A. Altecór, Y. Mao and K. Lozano: 'Large-scale synthesis of tin-doped indium oxide nanofibers using water as solvent', *Funct. Mater. Lett.*, **2012**, **05**, (03), 1250020.
- 63 Z. McEachin and K. Lozano: 'Production and characterization of polycaprolactone nanofibers via forspinning™ technology', *J. Appl. Polym. Sci.*, **2012**, **126**, (2), 473–479.
- 64 S. Padron, R. Patlan, J. Gutierrez, N. Santos, T. Eubanks and K. Lozano: 'Production and characterization of hybrid BEH-PPV/PEO conjugated polymer nanofibers by Forspinning™', *J. Appl. Polym. Sci.*, **2012**, **125**, (5), 3610–3616.
- 65 K. Shanmuganathan, Y. Fang, D. Y. Chou, S. Sparks, J. Hibbert and C. J. Ellison: 'Solventless high throughput manufacturing of poly(butylene terephthalate) nanofibers', *ACS Macro Lett.*, **2012**, **1**, (8), 960–964.
- 66 B. Vazquez, H. Vasquez and K. Lozano: 'Preparation and characterization of polyvinylidene fluoride nanofibrous membranes by Forspinning', *Polym. Eng. Sci.*, **2012**, **52**, (10), 2260–2265.
- 67 Y. Lu, Y. Li, S. Zhang, G. Xu, K. Fu, H. Lee and X. Zhang: 'Parameter study and characterization for polyacrylonitrile nanofibers fabricated via centrifugal spinning process', *Eur. Polymer J.*, **2013**, **49**, (12), 3834–3845.
- 68 L. Amalorpava Mary, T. Senthilram, S. Suganya, L. Nagarajan, J. Venugopal, S. Ramakrishna and V. R. Giri Dev: 'Centrifugal spun ultrafine fibrous web as a potential drug delivery vehicle', *Exp. Polym. Lett.*, **2013**, **7**, (3), 238–248.
- 69 B. Raghavan, H. Soto and K. Lozano: 'Fabrication of melt spun polypropylene nanofibers by Forspinning', *J. Eng. Fibers Fabr.*, **2013**, **8**, (1), 52–60.
- 70 Y. Rane, A. Altecór, N. S. Bell and K. Lozano: 'Preparation of superhydrophobic Teflon AF 600 sub-micron fibers and yarns using the Forspinning technique', *J. Eng. Fibers Fabr.*, **2013**, **8**, (4), 88–95.
- 71 L. Ren, V. Pandit, J. Elkin, T. Denman, J. A. Cooper and S. P. Kotha: 'Large-scale and highly efficient synthesis of micro- and nano-fibers



- with controlled fiber morphology by centrifugal jet spinning for tissue regeneration', *Nanoscale*, **2013**, **5**, (6), 2337–2345.
- 72 I. Sebe, B. Szabó, Z. K. Nagy, D. Szabó, L. Zsidai, B. Kocsis and R. Zelkó: 'Polymer structure and antimicrobial activity of polyvinylpyrrolidone-based iodine nanofibers prepared with high-speed rotary spinning technique', *Int. J. Pharm.*, **2013**, **458**, (1), 99–103.
  - 73 H. M. Golecki, H. Yuan, C. Glavin, B. Potter, M. R. Badrossamay, J. A. Goss, M. D. Phillips and K. K. Parker: 'Effect of solvent evaporation on fiber morphology in rotary jet spinning', *Langmuir*, **2014**, **30**, (44), 13369–13374.
  - 74 T. O'Haire, M. L. A. Rigout, S. J. Russell and C. M. Carr: 'Influence of nanotube dispersion and spinning conditions on nanofibre nanocomposites of polypropylene and multi-walled carbon nanotubes produced through Forcespinning', *J. Thermoplast. Compos. Mater.*, **2014**, **27**, (2), 205–214.
  - 75 B. Weng, F. Xu, A. Salinas and K. Lozano: 'Mass production of carbon nanotube reinforced poly(methyl methacrylate) nonwoven nanofiber mats', *Carbon*, **2014**, **75**, 217–226.
  - 76 N. E. Zander: 'Formation of melt and solution spun polycaprolactone fibers by centrifugal spinning', *J. Appl. Polym. Sci.*, **2015**, **132**, (2), 9.
  - 77 V. A. Agubra, D. De la Garza, L. Gallegos and M. Alcoutlabi: 'Forcespinning of polyacrylonitrile for mass production of lithium-ion battery separators', *J. Appl. Polym. Sci.*, **2016**, **133**, (1), 42847.
  - 78 B. Yang, C. L. H. Chen, J. Sun and H. Xu: 'Effective method for high-throughput manufacturing of ultrafine fibres via needleless centrifugal spinning', *Micro Nano Lett.*, **2015**, **10**, (2), 81–84.
  - 79 M. Krifa and W. Yuan: 'Morphology and pore size distribution of electrospun and centrifugal forcespun nylon 6 nanofiber membranes', *Text. Res. J.*, **2015**, **86**, (12), 1294–1306.
  - 80 X. Li, H. Chen and B. Yang: 'Centrifugally spun starch-based fibers from amylopectin rich starches', *Carbohydr. Polym.*, **2015**, **137**, 459–465.
  - 81 A. Salinas, M. Lizcano and K. Lozano: 'Synthesis of beta-SiC fine fibers by the forcespinning method with microwave irradiation', *J. Ceram.*, **2015**, **2015**, 5.
  - 82 M. Schabikowski, J. Tomaszewska, D. Kata and T. Graule: 'Rotary jet spinning of hematite fibers', *Text. Res. J.*, **2015**, **85**, (3), 316–324.
  - 83 A. Valipouri, S. A. H. Ravandi, A. Pishavar and E. I. Páráu: 'Experimental and numerical study on isolated and non-isolated jet behavior through centrifuge spinning system', *Int. J. Multiph. Flow*, **2015**, **69**, 93–101.
  - 84 B. Weng, F. Xu, G. Garza, M. Alcoutlabi, A. Salinas and K. Lozano: 'The production of carbon nanotube reinforced poly(vinyl) butyral nanofibers by the Forcespinning method', *Polym. Eng. Sci.*, **2015**, **55**, (1), 81–87.
  - 85 M. Yanilmaz and X. Zhang: 'Polymethylmethacrylate/polyacrylonitrile membranes via centrifugal spinning as separator in Li-ion batteries', *Polymers*, **2015**, **7**, (4), 629–643.
  - 86 H. A. Liu, D. Zepeda, J. P. Ferraris and K. J. J. Balkus: 'Electrospinning of poly(alkoxyphenylenevinylene) and methanofullerene nanofiber blends', *ACS Appl. Mater. Interfaces*, **2009**, **1**, (9), 1958–1965.
  - 87 S.-Y. Tsou, H.-S. Lin, P.-J. Cheng, C.-L. Huang, J.-Y. Wu and C. Wang: 'Rheological aspect on electrospinning of polyamide 6 solutions', *Eur. Polymer J.*, **2013**, **49**, (11), 3619–3629.
  - 88 E. Smit, U. Büttner and R. D. Sanderson: 'Continuous yarns from electrospun fibers', *Polymer*, **2005**, **46**, (8), 2419–2423.
  - 89 E. S. Cozza, Q. Ma, O. Monticelli and P. Cebe: 'Nanostructured nanofibers based on PBT and POSS: Effect of POSS on the alignment and macromolecular orientation of the nanofibers', *Eur. Polymer J.*, **2013**, **49**, (1), 33–40.
  - 90 Z. Ma, M. Kotaki, T. Yong, W. He and S. Ramakrishna: 'Surface engineering of electrospun polyethylene terephthalate (PET) nanofibers towards development of a new material for blood vessel engineering', *Biomaterials*, **2005**, **26**, (15), 2527–2536.
  - 91 C. M. Vaz, S. van Tuijl, C. V. C. Bouten and F. P. T. Baaijens: 'Design of scaffolds for blood vessel tissue engineering using a multi-layering electrospinning technique', *Acta Biomater.*, **2005**, **1**, (5), 575–582.
  - 92 F. Yang, R. Murugan, S. Wang and S. A. Ramakrishna: 'Electrospinning of nano/micro scale poly(l-lactic acid) aligned fibers and their potential in neural tissue engineering', *Biomaterials*, **2005**, **26**, (15), 2603–2610.
  - 93 H. Bai, L. Zhao, C. Lu, C. Li and G. Shi: 'Composite nanofibers of conducting polymers and hydrophobic insulating polymers: Preparation and sensing applications', *Polymer*, **2009**, **50**, (14), 3292–3301.
  - 94 D. Cho, H. Zhou, Y. Cho, D. Audus and Y. L. Joo: 'Structural properties and superhydrophobicity of electrospun polypropylene fibers from solution and melt', *Polymer*, **2010**, **51**, (25), 6005–6012.
  - 95 D. Aussawasathien, J. Dong and L. Dai: 'Electrospun polymer nanofiber sensors', *Synth. Met.*, **2005**, **154**, (1–3), 37–40.
  - 96 L.-J. Chen, J.-D. Liao, S.-J. Lin, Y.-J. Chuang and Y.-S. Fu: 'Synthesis and characterization of PVB/silica nanofibers by electrospinning process', *Polymer*, **2009**, **50**, (15), 3516–3521.
  - 97 A. Wilson, 'Nonwoven Filter Media: Technologies and Global Markets – AVM043E', BCC Research, **2015**.
  - 98 J. Pelipenko, P. Kocbek and J. Kristl: 'Critical attributes of nanofibers: preparation, drug loading, and tissue regeneration', *Int. J. Pharm.*, **2015**, **484**, (1–2), 57–74.
  - 99 R. Langer and J. P. Vacanti: 'Tissue engineering', *Science*, **1993**, **260**, (5110), 920–926.
  - 100 S. Agarwal, J. H. Wendorff and A. Greiner: 'Progress in the field of electrospinning for tissue engineering applications', *Adv. Mater.*, **2009**, **21**, (32–33), 3343–3351.
  - 101 L. Nagarajan and N. Gayathri: 'Production of nanofibres using rotary jet spinning method for tissue engineering', *Int. J. Sci. Res.*, **2016**, **5**, 858–864.
  - 102 X. Zhang, M. A. Geven, D. W. Grijpma, J. E. Gautrot and T. Peijs: 'Polymer-polymer composites for the design of strong and tough degradable biomaterials', *Mater. Today Commun.*, **2016**, **8**, 53–63.
  - 103 L. Cai and S. C. Heilshorn: 'Designing ECM-mimetic materials using protein engineering', *Acta Biomater.*, **2014**, **10**, (4), 1751–1760.
  - 104 M. Buzgo, M. Rampichova, K. Vocetkova, V. Sovkova, V. Lukasova, M. Doupnik, A. Mickova, F. Rustichelli and E. Amler: 'Emulsion centrifugal spinning for production of 3D drug releasing nanofibres with core/shell structure', *RSC Adv.*, **2017**, **7**, (3), 1215–1228.
  - 105 C. P. Barnes, S. A. Sell, E. D. Boland, D. G. Simpson and G. L. Bowlin: 'Nanofiber technology: designing the next generation of tissue engineering scaffolds', *Adv. Drug Deliv. Rev.*, **2007**, **59**, (14), 1413–1433.
  - 106 M. Rampichová, M. Buzgo, A. Mičková, K. Vocetková, V. Sovková, V. Lukášová, E. Filová, F. Rustichelli and E. Amler: 'Platelet-functionalized three-dimensional poly-epsilon-caprolactone fibrous scaffold prepared using centrifugal spinning for delivery of growth factors', *Int. J. Nanomed.*, **2017**, **12**, 347–361.
  - 107 J. Zhu, J. Yang and G. Sun: 'Cibacron blue F3GA functionalized poly(vinyl alcohol-co-ethylene) (PVA-co-PE) nanofibrous membranes as high efficient affinity adsorption materials', *J. Membr. Sci.*, **2011**, **385–386**, 269–276.
  - 108 J. Ma, J. Meng, M. Simonet, N. Stingelin, T. Peijs and G. B. Sukhorukov: 'Biodegradable fibre scaffolds incorporating water-soluble drugs and proteins', *J. Mater. Sci. Mater. Med.*, **2015**, **26**, (7), 205.
  - 109 S. Marano, S. A. Barker, B. T. Raimi-Abraham, S. Missaghi, A. Rajabi-Siahboomi and D. Q. M. Craig: 'Development of micro-fibrous solid dispersions of poorly water-soluble drugs in sucrose using temperature-controlled centrifugal spinning', *Eur. J. Pharm. Biopharm.*, **2016**, **103**, 84–94.
  - 110 L. Wang, M.-W. Chang, Z. Ahmad, H. Zheng and J.-S. Li: 'Mass and controlled fabrication of aligned PVP fibers for matrix type antibiotic drug delivery systems', *Chem. Eng. J.*, **2016**, **307**, 661–669.
  - 111 G. Mehetre, V. Pande and P. Kendre: 'An overview of nanofibers as a platform for drug delivery', *NDDS*, **2015**, **2015**, (3), 1–5.
  - 112 U. Stachewicz, F. Modaresifar, R. J. Bailey, T. Peijs and A. H. Barber: 'Manufacture of void-free electrospun polymer nanofiber composites with optimized mechanical properties', *ACS Appl. Mater. Interfaces*, **2012**, **4**, (5), 2577–2582.
  - 113 H. Zhang, A. Bharti, Z. Li, S. Du, E. Bilotti and T. Peijs: 'Localized toughening of carbon/epoxy laminates using dissolvable thermoplastic interleaves and electrospun fibres', *Compos. Part A: Appl. Sci. Manuf.*, **2015**, **79**, 116–126.
  - 114 H. Zhang, Y. Liu, M. Kuwata, E. Bilotti and T. Peijs: 'Improved fracture toughness and integrated damage sensing capability by spray coated CNTs on carbon fibre prepreg', *Compos. Part A: Appl. Sci. Manuf.*, **2015**, **31**, (70), 102–110.
  - 115 Q. Chen, W. D. Wu, Y. Zhao, M. Xi, T. Xu and H. Fong: 'Nano-epoxy resins containing electrospun carbon nanofibers and the resulting hybrid multi-scale composites', *Compos. Part B-Eng.*, **2014**, **58**, 43–53.
  - 116 G. A. Tanami, E. Wachtel and G. Marom: 'Crystalline structure and thermodynamic analysis of ultra-low diameter VGCF-polypropylene nanocomposite monofilaments', *Polym. Compos.*, **2016**, **37**, (6), 1641–1649.
  - 117 Y. K. Choi, K. Sugimoto, S. M. Song, Y. Gotoh, Y. Ohkoshi and M. Endo: 'Mechanical and physical properties of epoxy composites reinforced by vapor grown carbon nanofibers', *Carbon*, **2005**, **43**, (10), 2199–2208.



- 118 S. J. Eichhorn, A. Dufresne, M. Aranguren, N. E. Marcovich, J. R. Capadona, S. J. Rowan, C. Weder, W. Thielemans, M. Roman, S. Renneckar, W. Gindl, S. Veigel, J. Keckes, H. Yano, K. Abe, M. Nogi, A. N. Nakagaito, A. Mangalam, J. Simonsen, A. S. Benight, A. Bismarck, L. A. Berglund and T. Peijs: 'Review: current international research into cellulose nanofibres and nanocomposites', *J. Mater. Sci.*, **2009**, **45**, (1), 1–33.
- 119 M. H. Al-Saleh and U. Sundararaj: 'A review of vapor grown carbon nanofiber/polymer conductive composites', *Carbon*, **2009**, **47**, (1), 2–22.
- 120 F. Hussain, M. Hojjati, M. Okamoto and R. E. Gorga: 'Review article: polymer-matrix nanocomposites, processing, manufacturing, and application: An overview', *J. Compos. Mater.*, **2006**, **40**, (17), 1511–1575.
- 121 T. Peijs, 'Electrospun polymer nanofibers and their composites' In: Reference Module in Materials Science and Materials Engineering, Comprehensive Composite Materials II, Vol. 6, Chap. 6.7, **2018**, pp. 162–200.
- 122 Q. Chen, L. Zhang, M.-K. Yoon, X.-F. Wu, R. H. Arefin and H. Fong: 'Preparation and evaluation of nano-epoxy composite resins containing electrospun glass nanofibers', *J. Appl. Polym. Sci.*, **2012**, **124**, (1), 444–451.
- 123 E. Bafekrpour, C. Yang, M. Natali and B. Fox: 'Functionally graded carbon nanofiber/phenolic nanocomposites and their mechanical properties', *Compos. Part A: Appl. Sci. Manuf.*, **2013**, **54**, 124–134.
- 124 D. Kai, M. P. Prabhakaran, B. Stahl, M. Eblenkamp, E. Wintermantel and S. Ramakrishna: 'Mechanical properties and in vitro behavior of nanofiber-hydrogel composites for tissue engineering applications', *Nanotechnology*, **2012**, **23**, (9), 095705.
- 125 L. Daelemans, S. V. D. Heijden, I. D. Baere, H. Rahier, W. V. Paepegem and K. D. Clerck: 'Damage-resistant composites using electrospun nanofibers: A multiscale analysis of the toughening mechanisms', *ACS Appl. Mater. Interfaces*, **2016**, **8**, (18), 11806–11818.
- 126 D. Papkov, Y. Zou, M. N. Andalib, A. Goponenko, S. Z. D. Cheng and Y. A. Dzenis: 'Simultaneously strong and tough ultrafine continuous nanofibers', *ACS Nano*, **2013**, **7**, (4), 3324–3331.
- 127 J. Yao, G. Li, C. W. M. Bastiaansen and T. Peijs: 'High performance copolyimide nanofiber reinforced composites', *Polymer*, **2015**, **76**, 46–51.
- 128 M. R. Badrossamay, K. Balachandran, A. K. Capulli, H. M. Golecki, A. Agarwal, J. A. Goss, H. Kim, K. Shin and K. K. Parker: 'Engineering hybrid polymer-protein super-aligned nanofibers via rotary jet spinning', *Biomaterials*, **2014**, **35**, (10), 3188–3197.
- 129 A. E. Erickson, D. Edmondson, F.-C. Chang, D. Wood, A. Gong, S. L. Levengood and M. Zhang: 'High-throughput and high-yield fabrication of uniaxially-aligned chitosan-based nanofibers by centrifugal electrospinning', *Carbohydr. Polym.*, **2015**, **134**, 467–474.
- 130 K. Sutherland: 'Filters and filtration handbook', 5th edn; **2008**, Oxford, Elsevier.
- 131 K. Yoon, B. S. Hsiao and B. Chu: 'Functional nanofibers for environmental applications', *J. Mater. Chem.*, **2008**, **18**, (44), 5326–5334.
- 132 Y. C. Ahn, S. K. Park, G. T. Kim, Y. J. Hwang, C. G. Lee, H. S. Shin and J. K. Lee: 'Development of high efficiency nanofilters made of nanofibers', *Curr. Appl. Phys.*, **2006**, **6**, (6), 1030–1035.
- 133 A. Podgórski, A. Bałazy and L. Gradoń: 'Application of nanofibers to improve the filtration efficiency of the most penetrating aerosol particles in fibrous filters', *Chem. Eng. Sci.*, **2006**, **61**, (20), 6804–6815.
- 134 S. Virji, J. Huang, R. B. Kaner and B. H. Weiller: 'Polyaniline nanofiber gas sensors: examination of response mechanisms', *Nano Lett.*, **2004**, **4**, (3), 491–496.
- 135 S. Berson, R. De Bettignies, S. Bailly and S. Guillerez: 'Poly(3-hexylthiophene) fibers for photovoltaic applications', *Adv. Func. Mater.*, **2007**, **17**, (8), 1377–1384.
- 136 Q. Wu, Y. Xu, Z. Yao, A. Liu and G. Shi: 'Supercapacitors based on flexible graphene/polyaniline nanofiber composite films', *ACS Nano*, **2010**, **4**, (4), 1963–1970.
- 137 K. Zhang, L. L. Zhang, X. S. Zhao and J. Wu: 'Graphene/polyaniline nanofiber composites as supercapacitor electrodes', *Chem. Mat.*, **2010**, **22**, (4), 1392–1401.
- 138 V. A. Agubra, L. Zuniga, D. Flores, H. Campos, J. Villarreal and M. Alcoutlabi: 'A comparative study on the performance of binary SnO<sub>2</sub>/NiO/C and Sn/C composite nanofibers as alternative anode materials for lithium ion batteries', *Electrochim. Acta*, **2017**, **224**, 608–621.
- 139 H. Tsuchida, R. Nakamura, K. Kinashi, W. Sakai, N. Tsutsumi, M. Ozaki and T. Okabe: 'Radiation-induced colour changes in a spiropyran/BaFCl:Eu<sup>2+</sup>/polystyrene composite film and nonwoven fabric', *New J. Chem.*, **2016**, **40**, (10), 8658–8663.
- 140 C. Liang, C. Hu, K. Yan, H. Thomas and X. Zhu: 'Hydrophilic nonwovens by Forcespinning™ of isotactic polypropylene blended with amphiphilic surfactants', *Fiber. Polym.*, **2016**, **17**, (10), 1646–1656.
- 141 R. Ou, J. Wei, L. Jiang, G. P. Simon and H. Wang: 'Robust thermoresponsive polymer composite membrane with switchable superhydrophilicity and superhydrophobicity for efficient oil-water separation', *Environ. Sci. Technol.*, **2016**, **50**, 906–914.
- 142 G. L. Dotto, J. M. N. D. Santos, E. Tanabe, D. A. Bertuol, E. L. Foletto, E. C. Lima and F. A. Pavan: 'Chitosan/polyamide nanofibers prepared by Forcespinning technology: A new adsorbent to remove anionic dyes from aqueous solutions', *J. Clean. Prod.*, **2017**, **144**, 120–129.
- 143 S. Ramakrishna, K. Fujihara, W.-E. Teo, T. Yong, Z. Ma and R. Ramaseshan: 'Electrospun nanofibers: solving global issues', *Mater. Today*, **2006**, **9**, (3), 40–50.
- 144 N. Obregon, V. Agubra, M. Pokhrel, H. Campos, D. Flores, D. De la Garza, Y. Mao, J. Macossay and M. Alcoutlabi: 'Effect of polymer concentration, rotational speed, and solvent mixture on fiber formation using Forcespinning', *Fibers*, **2016**, **4**, (2), 20.
- 145 B. Weng, F. Xu and K. Lozano: 'Mass production of carbon nanotube-reinforced polyacrylonitrile fine composite fibers', *J. Appl. Polym. Sci.*, **2014**, **131**, (11), 40302.
- 146 T. B. Mindru, L. Ignat, I. B. Mindru and M. Pinteala: 'Morphological aspects of polymer fiber mats obtained by air flow rotary-jet spinning', *Fiber. Polym.*, **2013**, **14**, (9), 1526–1534.
- 147 M. A. Hammami, M. Krifa and O. Harzallah: 'Centrifugal force spinning of PA6 nanofibers – processability and morphology of solution-spun fibers', *J. Text. Inst.*, **2014**, **105**, (6), 637–647.
- 148 M. Krifa, M. A. Hammami and H. Wu: 'Occurrence and morphology of bead-on-string structures in centrifugal forcespun PA6 fibers', *J. Text. Inst.*, **2015**, **106**, (3), 284–294.
- 149 S. Khan, M. Ul-Islam, M. W. Ullah, M. Ikram, F. Subhan, Y. Kim, J. H. Jang, S. Yoon and J. K. Park: 'Engineered regenerated bacterial cellulose scaffolds for application in in vitro tissue regeneration', *RSC Adv.*, **2015**, **5**, 84565–84573.
- 150 V. A. Agubra, L. Zuniga, D. De la Garza, L. Gallegos, M. Pokhrel and M. Alcoutlabi: 'Forcespinning: a new method for the mass production of Sn/C composite nanofiber anodes for lithium ion batteries', *Solid State Ionics*, **2016**, **286**, 72–82.
- 151 S. D. Mohan, G. R. Mitchell and F. J. Davis: 'Development of molecular anisotropy in centrifugally spun fibers as compared to electrospun fibers', *Macromol. Mater. Eng.*, **2016**, **301**, (11), 1313–1319.
- 152 A. Salinas, A. Altecór, M. Lizcano and K. Lozano: 'Production of beta-silicon carbide nanofibers using the Forcespinning method', *J. Ceram. Sci. Technol.*, **2016**, **7**, (3), 229–234.
- 153 A. Amir, S. Mahalingam, X. Wu, H. Porwal, P. Colombo, M. J. Reece and M. Edirisinghe: 'Graphene nanoplatelets loaded polyurethane and phenolic resin fibres by combination of pressure and gyration', *Compos. Sci. Technol.*, **2016**, **129**, 173–182.
- 154 W. Xu, L. Xia, J.-G. Ju, P. Xi, B.-W. Cheng and Y.-X. Liang: 'Preparation and low-temperature gas-sensing properties of SnO<sub>2</sub> ultra-fine fibers fabricated by a centrifugal spinning process', *J. Sol-Gel Sci. Technol.*, **2016**, **78**, 353–364.
- 155 R. Nava, L. D. Cremer, V. Agubra, J. Sanchez, M. Alcoutlabi and K. Lozano: 'Centrifugal spinning: an alternative for large scale production of silicon-carbon composite nanofibers for lithium ion batteries anodes', *ACS Appl. Mater. Interfaces*, **2016**, **8**, 29365–29372.
- 156 V. Agubra, L. Zuniga, D. Flores and M. Alcoutlabi: 'Forcespinning of microfibers and their applications in lithium-ion and sodium-ion batteries', *ECS Trans.*, **2016**, **72**, (8), 57–65.
- 157 H. Chen, X. Li, N. Li and B. Yang: 'Electrostatic-assisted centrifugal spinning for continuous collection of submicron fibers', *Text. Res. J.*, **2016**, **87**, 2349–2357.
- 158 T. Hou, X. Li, Y. Lu and B. Yang: 'Highly porous fibers prepared by centrifugal spinning', *Mater. Design*, **2017**, **114**, 303–311.
- 159 L. F. Deravi, N. R. Sinatra, C. O. Chantre, A. P. Nesmith, H. Yuan, S. K. Deravi, J. A. Goss, L. A. MacQueen, M. R. Badrossamay, G. M. Gonzalez, M. D. Phillips and K. K. Parker: 'Design and fabrication of fibrous nanomaterials using pull spinning', *Macromol. Mater. Eng.*, **2017**, **302**, 1600404.
- 160 M. Dinkgreve, M. M. Denn and D. Bonn: 'Everything flows: Elastic effects on startup flows of yield-stress fluids', *Rheol. Acta*, **2017**, **56**, 189–194.
- 161 K. Dassios: 'Modification of carbon fibre/epoxy composites by polyvinylalcohol (PVA) based electrospun nanofibres', *Adv. Compos. Lett.*, **2017**, **25**, 69–76.
- 162 S. van der Heijden, L. Daelemans, K. De Bruycker, R. Simal, I. De Baere, W. Van Paepegem, H. Rahier and K. De Clerck: 'Novel composite materials with tunable delamination resistance using functionalizable electrospun SBS fibers', *Compos. Struct.*, **2017**, **159**, 12–20.

- 163 D. N. Riahi: 'Modeling and computation of nonlinear rotating polymeric jets during forspinning process', *Int. J. Non-Linear Mech.*, **2017**, **92**, 1–7.
- 164 S. J. Upson, T. O'Haire, S. J. Russell, K. Dalgarno and A. M. Ferreira: 'Centrifugally spun PHBV micro and nanofibres', *Mater. Eng. C*, **2017**, **76**, 190–195.
- 165 X. Hong, S. Mahalingam and M. Edirisinghe: 'Simultaneous application of pressure-infusion-gyration to generate polymeric nanofibers', *Macromol. Mater. Eng.*, **2017**, **302**, 1600564.
- 166 X. Lin, B. Liu, X. Wang, L. Zhu, X. Jin, X. Liu, G. Zhang and D. Xu: 'Large scale fabrication of magnesium oxide fibers for high temperature thermal structure applications', *Ceram. Int.*, **2016**, **43**, 1455–1459.
- 167 Q. Zhang, N. Bao, X. Wang, X. Hu, X. Miao, M. Chaker and D. Ma: 'Advanced fabrication of chemically bonded graphene/TiO<sub>2</sub> continuous fibers with enhanced broadband photocatalytic properties and involved mechanisms exploration', *Sci. Rep.*, **2016**, **6**, 38066.
- 168 Z. Xu, S. Mahalingam, P. Basnett, B. Raimi-Abraham, I. Roy, D. Craig and M. Edirisinghe: 'Making nonwoven fibrous poly( $\epsilon$ -caprolactone) constructs for antimicrobial and tissue engineering applications by pressurized melt gyration', *Macromol. Mater. Eng.*, **2016**, **301**, 922–934.
- 169 P. Mellado, H. A. McIlwee, M. R. Badrossamay, J. A. Goss, L. Mahadevan and K. Kit Parker: 'A simple model for nanofiber formation by rotary jet-spinning', *Appl. Phys. Lett.*, **2011**, **99**, (20), 203107.
- 170 S. Mahalingam and M. Edirisinghe: 'Forming of polymer nanofibers by a pressurised gyration process', *Macromol. Rapid Commun.*, **2013**, **34**, (14), 1134–1139.
- 171 S. Mahalingam, G. Ren and M. Edirisinghe: 'Rheology and pressurised gyration of starch and starch-loaded poly(ethylene oxide)', *Carbohydr. Polym.*, **2014**, **114**, 279–287.
- 172 C. Feng, X. Lin, X. Wang, H. Liu, B. Liu, L. Zhu, G. Zhang and D. Xu: 'Preparation, ferromagnetic and photocatalytic performance of NiO and hollow Co<sub>3</sub>O<sub>4</sub> fibers through centrifugal-spinning technique', *Mater. Res. Bull.*, **2016**, **74**, 319–324.
- 173 E. Tan and C. T. Lim: 'Mechanical characterization of nanofibers: A review', *Compos. Sci. Technol.*, **2006**, **66**, 1102–1111.
- 174 E. Tan, C. N. Goh, C. H. Sow and C. T. Lim: 'Tensile test of a single nanofiber using an atomic force microscope tip', *Appl. Phys. Lett.*, **2005**, **86**, (7), 073115.
- 175 F. Hang, D. Lu, R. J. Bailey, I. Jimenez-Palomar, U. Stachewicz, B. Cortes-Ballesteros, M. Davies, M. Zech, C. Bödefeld and A. H. Barber: 'In situ tensile testing of nanofibers by combining atomic force microscopy and scanning electron microscopy', *Nanotechnology*, **2011**, **22**, (36), 365708.
- 176 L.-Q. Liu, D. Tasis, M. Prato and H. D. Wagner: 'Tensile mechanics of electrospun multiwalled nanotube/poly(methyl methacrylate) nanofibers', *Adv. Mater.*, **2007**, **19**, (9), 1228–1233.
- 177 W. Wang, P. Ciselii, E. V. Kuznetsov, T. Peijs and A. H. Barber: 'Effective reinforcement in carbon nanotube-polymer composites', *Philos. Trans. A Math. Phys. Eng. Sci.*, **2008**, **366**, (1870), 1613–1626.
- 178 K. Y. Hwang, S.-D. Kim, Y.-W. Kim and W.-R. Yu: 'Mechanical characterization of nanofibers using a nanomanipulator and atomic force microscope cantilever in a scanning electron microscope', *Polym. Test.*, **2010**, **29**, 375–380.
- 179 S. R. Baker, S. Banerjee, K. Bonin and M. Guthold: 'Determining the mechanical properties of electrospun poly- $\epsilon$ -caprolactone (PCL) nanofibers using AFM and a novel fiber anchoring technique', *Mater. Sci. Eng. C*, **2016**, **59**, 203–212.
- 180 E. Tan, S. Ng and C. Lim: 'Tensile testing of a single ultrafine polymeric fiber', *Biomaterials*, **2005**, **26**, 1453–1456.
- 181 A. Arinstein, M. Burman, O. Gendelman and E. Zussman: 'Effect of supramolecular structure on polymer nanofibre elasticity', *Nat. Nanotechnol.*, **2007**, **2**, (1), 59–62.
- 182 J. Yao, M. F. Pantano, N. M. Pugno, C. W. M. Bastiaansen and T. Peijs: 'High-performance electrospun co-polyimide nanofibers', *Polymer*, **2015**, **76**, 105–112.
- 183 H. E. Daniels: 'The statistical theory of the strength of bundles of threads', I. In: *Proc. Royal Soc. London A: Math., Phys. Engin. Sci.*, **1945**, **183**, (995), 405–435.
- 184 F. Chen, X. Peng, T. Li, S. Chen, X.-F. Wu, D. H. Reneker and H. Hou: 'Mechanical characterization of single high-strength electrospun polyimide nanofibers', *J. Phys. D: Appl. Phys.*, **2008**, **41**, (2), 025308.
- 185 Y. Zhou, J. Fang, X. Wang and T. Lin: 'Strip twisted electrospun nanofiber yarns: structural effects on tensile properties', *J. Mater. Res.*, **2012**, **27**, (03), 537–544.
- 186 S. P. Decent, A. C. King, M. J. H. Simmons, E. I. Părău, I. M. Wallwork, C. J. Gurney and J. Uddin: 'The trajectory and stability of a spiralling liquid jet: Viscous theory', *Appl. Math. Model.*, **2009**, **33**, (12), 4283–4302.
- 187 E. I. Părău, S. P. Decent, M. J. H. Simmons, D. Wong and A. C. King: 'Nonlinear viscous liquid jets from a rotating orifice', *J. Eng. Math.*, **2006**, **57**, (2), 159–179.
- 188 G. H. McKinley: 'Visco-elasto-capillary thinning and break-up of complex fluids', *Rheology Reviews*, **2005**, 1–48.
- 189 G. H. McKinley and T. Sridhar: 'Filament-stretching rheometry of complex fluids', *Annu. Rev. Fluid Mech.*, **2002**, **34**, (1), 375–415.
- 190 V. Tirtaatmadja, G. H. McKinley and J. J. Cooper-White: 'Drop formation and breakup of low viscosity elastic fluids: Effects of molecular weight and concentration', *Phys. Fluids*, **2006**, **18**, (4), 043101.
- 191 C. Wagner, L. Bourouiba and G. H. McKinley: 'An analytic solution for capillary thinning and breakup of FENE-P fluids', *J. Non-Newton. Fluid Mech.*, **2015**, **218**, 53–61.
- 192 C. J. Thompson, G. G. Chase, A. L. Yarin and D. H. Reneker: 'Effects of parameters on nanofiber diameter determined from electrospinning model', *Polymer*, **2007**, **48**, (23), 6913–6922.
- 193 I. M. Wallwork, S. P. Decent, A. C. King and R. M. S. M. Schulkes: 'The trajectory and stability of a spiralling liquid jet. Part 1. Inviscid theory', *J. Fluid Mech.*, **2002**, **459**, 43–65.
- 194 A. Valipouri, S. Abdolkarim, H. Ravandi, A. Pishevar and I. P. Emilian: 'Numerical study on the jet dynamic through centrifuge spinning: Influence of angular velocity', *J. Text. Polym.*, **2015**, **3**, 20–25.
- 195 S. L. Shenoy, W. D. Bates, H. L. Frisch and G. E. Wnek: 'Role of chain entanglements on fiber formation during electrospinning of polymer solutions: Good solvent, non-specific polymer-polymer interaction limit', *Polymer*, **2005**, **46**, (10), 3372–3384.
- 196 R. H. Colby, L. J. Fetters and W. W. Graessley: 'The melt viscosity-molecular weight relationship for linear polymers', *Macromolecules*, **1987**, **20**, (9), 2226–2237.
- 197 D. K. Thomas and T. A. J. Thomas: 'Viscosity-concentration relationships in solutions of high polymers', *J. Appl. Polym. Sci.*, **1960**, **3**, (8), 129–131.
- 198 M. S. N. Oliveira, R. Yeh and G. H. McKinley: 'Iterated stretching, extensional rheology and formation of beads-on-a-string structures in polymer solutions', *J. Nonnewton. Fluid Mech.*, **2006**, **137**, (1–3), 137–148.
- 199 S. Padron, D. I. Caruntu and K. Lozano: 'On 2D Forcespinning modeling', *Proc. ASME Inter. Mech. Engin. Congress and Exposition*, **2011**, **7**, Pts A and B, 821–830.
- 200 V. Gowariker, V. N. Krishnamurthy, S. Gowariker, M. Dhanorkar and K. Paranjape: 'The fertilizer encyclopedia', John Wiley & Sons, Hoboken, New Jersey, **2009**.
- 201 A. C. Pipkin: 'Lectures on viscoelasticity theory', **1986**, New York, Springer.
- 202 M. Parthasarathy and D. J. Klingenberg: 'Large amplitude oscillatory shear of ER suspensions', *J. Non-Newton. Fluid Mech.*, **1999**, **81**, (1–2), 83–104.
- 203 R. T. Weitz, L. Harnau, S. Rauschenbach, M. Burghard and K. Kern: 'Polymer nanofibers via nozzle-free centrifugal spinning', *Nano Lett.*, **2008**, **8**, (4), 1187–1191.
- 204 C. Angammana and S. Jayaram: 'A study of free surface electrospinning process to enhance and optimize the nanofiber production', *Proc. 2012 Electrostatics Joint Conference*, June, **2012**.
- 205 W.-M. Chang, C.-C. Wang and C.-Y. Chen: 'The combination of electrospinning and Forcespinning: Effects on a viscoelastic jet and a single nanofiber', *Chem. Eng. J.*, **2014**, **244**, 540–551.
- 206 B. Raimi-Abraham, S. Mahalingam, M. J. Edirisinghe and D. Q. M. Craig: 'Generation of poly(N-vinylpyrrolidone) nanofibers using pressurised gyration', *Mater. Sci. Eng. C Mater. Biol. Appl.*, **2014**, **39**, 168–176.
- 207 Z. Xu, S. Mahalingam, J. L. Rohn, G. Ren and M. Edirisinghe: 'Physio-chemical and antibacterial characteristics of pressure spun nylon nanofibres embedded with functional silver nanoparticles', *Mater. Sci. Eng. C Mater. Biol. Appl.*, **2015**, **56**, 195–204.
- 208 F. Brako, B. Raimi-Abraham, S. Mahalingam, D. Q. M. Craig and M. Edirisinghe: 'Making nanofibres of mucoadhesive polymer blends for vaginal therapies', *Eur. Polymer J.*, **2015**, **70**, 186–196.
- 209 S. Zhang, B. T. Karaca, S. K. VanOosten, E. Yuca, S. Mahalingam, M. Edirisinghe and C. Tamerler: 'Coupling infusion and gyration for the nanoscale assembly of functional polymer nanofibers integrated with genetically engineered proteins', *Macromol. Rapid Commun.*, **2015**, **36**, (14), 1322–1328.
- 210 S. Mahalingam, G. Pierin, P. Colombo and M. Edirisinghe: 'Facile one-pot formation of ceramic fibres from preceramic polymers by pressurised gyration', *Ceram. Int.*, **2015**, **41**, (4), 6067–6073.